Intershell interaction in atoms

M. Ya. Amus'ya and V. K. Ivanov

A. F. Ioffe Physicotechnical Institute, Academy of Sciences of the USSR, Leningrad

M. I. Kalinin Polytechnic Institute, Leningrad

Usp. Fiz. Nauk **152**, 185–230 (June 1987)

The fundamental results obtained in the past 10–15 years in studying the correlation intershell interaction in atoms are reviewed. Major attention is paid to photo processes in which the manifestations of intershell interaction have been studied both experimentally and theoretically to the greatest degree. The strong influence of multielectron shells on the few-electron shells is demonstrated with concrete examples by comparing the results of various calculations and the existing experimental data for the partial ionization cross sections, the angular distributions, and the degree of polarization of the photoelectrons. The general qualitative regularities of the manifestations of the intershell interaction and their differences in atoms with filled and unfilled shells are discussed. The processes of readjustment of the electron shells of an atom that arise from the appearance of a vacancy and their influence on the intershell interaction are examined. The literature is covered to April 1986.

TABLE OF CONTENTS

1. INTRODUCTION

Up to the middle 60s, the single-particle model predominated in the study of ionization of atoms, based on the concept of independent motion of the electrons in an atom.[1–5] The simplest variant of the single-particle model, the hydrogen-like approximation,[2,4] treats the motion of the electrons in the screened field of the nucleus, which retains its Coulomb nature. However, this approximation proves too crude, yielding a considerable error even in describing the positions of the levels in which the atomic electrons are situated.

The refinement of the mean field in which they move independently led to the devising of the most perfected variant of the single-particle model—the self-consistent-field approximation of Hartree and Fock.[1,4,5] The latter has enabled substantial advances in the description of the structure of atoms. In particular, values of the total energy and ionization potentials of the different subshells have been obtained within the framework of the Hartree-Fock approximation that are very close to the experimental values. It was possible, at least semiquantitatively, to describe the excitation and ionization probabilities of atoms (Ref. 4 and the references contained therein), as well as the energies and other characteristics of excited and ionized states.

In the 60s new experimental data revealed a set of features in the absorption spectra and ionization cross sections that were not explained within the framework of single-particle models, including the Hartree-Fock method. The further comparison of experiment with the most exact calculations of that time[4,6] showed the need for escaping the framework of the single-particle approximation. Moreover, as it turned out, the Hartree-Fock method has certain inner defects in describing ionization in that it violates the sum rules that are valid when describing an atom using exact wave functions.[5]

 0038-5670/87/060449-26$01.80

By definition, going outside the framework of the Hartree-Fock approximation implies taking account of many-electron correlations arising from the component of the electron–electron interaction that is neglected in defining the self-consistent mean field. It is natural to take account of this interaction, sometimes called the residual or indirect field, initially among the electrons of only a single shell,[1)] since the latter are well separated in space and energy. As applied to the study of processes of ionization and excitation of atoms, the correlations were first successfully taken into account within the framework of the approximation of random phases with exchange—the ARPE.[7] It was possible in these calculations,[7] and then by using other methods,[8–11] allowing for the residual interaction among the electrons of the shell being ionized, to obtain satisfactory agreement with the experimental data on the total photoionization cross sections in the region of energies of quanta from the ionization threshold to several hundred electron volts. It turned out that the residual interaction among the electrons is substantial for all outer and intermediate multielectron shells p^6, d^{10}, and f^{14}, which give the greatest contribution to the total photoionization cross section.

The next stage was to take account of the residual interaction of electrons belonging to different shells.[12,13] We call this interaction the intershell interaction, in contrast to that mentioned above, which was later termed the intrashell interaction. Although the atomic shells are well separated from one another, taking account of the coupling of electrons of different shells proves very important in describing a number of dynamic processes in an atom. The intershell interaction is manifested most strongly in the ionization cross sections of few-electron shells, in the total ionization cross sections at the thresholds of the inner shells, in the angular distribution and polarization of the photoelectrons, in the decay of vacancies in the inner shells, and in the photoelectron spectra. The prediction of a substantial effect of the multielectron shells on the few-electron shells,[12,13] the total loss by the latter of their individuality, and as a consequence, their collectivization, has served as an impetus to broad experimental and theoretical study of the manifestations of intershell interaction.

A large number of studies have been conducted up to now in this field of atomic physics, and an extensive material has been amassed that enables revealing the role and fundamental features of the manifestation of intershell interaction. The studies that have been performed have shown that it is substantial in all the atoms of the periodic system.

This review is devoted to presenting the fundamental results obtained in this field during the past 15 years. Main attention is paid to the dynamic processes in atoms in which the intershell interaction plays a decisive role and its manifestations are most significant. The energy structure of atoms is practically not discussed in the review, since intershell correlations generally play a smaller role in determining it (in particular, the energies of single-electron levels) than in determining the probabilities of transitions.

One can take account of the interaction between the shells of an atom by using a number of theoretical methods (see the review of Ref. 14). The widespread ones use the apparatus of many-body theory and apply the diagram technique,[15] i.e., the ARPE[7,16] and many-particle perturbation theory (MPT).[17,18] While based on the Hartree-Fock approximation as a zero-order approximation, the apparatus of many-body theory enables one to represent the mechanism of any process under study in the lowest nonvanishing order of perturbation theory with respect to the interelectron interaction and to represent the corrections to it in the higher orders.

In this review we shall use the apparatus of many-body theory.

To describe the phenomena associated with the fine structure of the levels and the polarization of the photoelectrons, we must allow for relativistic effects. The existing relativistic variants of the ARPE[19] and MPT[20] methods have substantially expanded the field of study of the intershell interaction (see Secs. 2.6, 4.2, and 4.4 below).

Among the other approaches we note the method traditional in atomic physics of configuration superposition and its different modifications: the multiconfiguration Hartree-Fock approximation,[21] the R-matrix approximation,[9] and the transition-matrix method.[22] The local-density approximation, which was borrowed from the theory of an inhomogeneous electron gas, has been developed recently in atomic calculations. Good results in studying atoms are obtained by using a variant of this method that takes account of the time-dependence of the electron density in ionization and excitation processes—the so-called time-dependent local-density approximation.[23] Some of the methods cited above also have relativistic generalizations.[24,25]

Simultaneously with the development of the theoretical approaches to atoms, and often overtaking them, the front of experimental studies has considerably expanded.[26] This has been facilitated by the appearance of new, powerful sources of continuous-spectrum radiation and by progress in the techniques and methodology of experimental measurements. All this enables one to obtain more reliable and detailed information on the structure of the atom.

In this review major attention is paid to intershell effects manifested in different photoprocesses, where they have been studied to the greatest degree, both theoretically and experimentally.

2. PARTIAL IONIZATION CROSS SECTIONS OF ATOMS WITH FILLED SHELLS

2.1. Determinations of the amplitude and photoionization cross section

Let us examine the photoionization amplitude and cross section with account taken of electron correlations. In Sec. 2 and below we shall use the atomic system of units: $\hbar = m_e = e = 1$.

In the region of energies of quanta

$$\omega = kc \ll \frac{c}{R_{nl}},$$

where k is the wave vector of the photon, c is the velocity of light, and R_{nl} is the effective radius of the shell being ionized, the dipole approximation is valid. The operator for the interaction of an atomic electron with the electromagnetic field in the dipole approximation is usually written in one of two equivalent forms—distance (r-form) and velocity (∇-form). The corresponding photoionization cross sections in the single-electron approximation have the form

$$\sigma_{im}^{r}(\omega) = 4\pi^2\alpha\omega \,|\, \mathbf{e}\langle m \,|\, \mathbf{r} \,|\, i\rangle \,|^2,$$
$$\sigma_{im}^{\nabla}(\omega) = \frac{4\pi^2\alpha}{\omega} \,|\, \mathbf{e}\langle m \,|\, \hat{\nabla} \,|\, i\rangle \,|^2. \qquad (2.1)$$

Here $\langle m|\mathbf{r}|i\rangle$ and $\langle m|\hat{\nabla}|i\rangle$ are the amplitudes of the dipole transitions of an electron from shell i to the state m, $\mathbf{e}$ is the polarization vector, $\alpha = 1/c \approx 1/137$, and $\omega = E_m - E_i$ (E_m and E_i are the energies of the states $\langle m|$ and $|i\rangle$).

In taking account of the residual interaction, one substitutes for the dipole matrix elements $\langle m|\mathbf{r}|i\rangle$ and $\langle m|\hat{\nabla}|i\rangle$ matrix elements which take into account the electron correlations, e.g., in the ARPE[16] or MPT[17] approximation.

The electrons of each shell having the quantum numbers n and l can undergo dipole transitions $nl \to n'l \pm 1$ to free states of the discrete or continuous spectra. The transition yielding the main contribution to the total photoionization cross section in the given energy region is called the "strong" transition, and the others "weak." The probability of photoionization of shells possessing "strong" transitions is substantially altered upon taking account of the interaction between the electrons of the given shell.[7,16] That is, the intrashell correlations are large for them, whereas the role of these correlations is usually small for shells with "weak" transitions.

The intrashell interaction is taken into account within the framework of the ARPE by solving the integral equation for the amplitude of the phototransition $n_1l_1 \to \varepsilon l$ (ε is the energy of the ejected electron)[7]:

$$\langle \varepsilon l \,|\, \hat{D}(\omega) \,|\, n_1l_1\rangle = \langle \varepsilon l \,|\, \hat{d} \,|\, n_1l_1\rangle$$
$$+ \left(\sum, \int\right)_{\varepsilon', l'} \left(\frac{\langle \varepsilon' l' \,|\, \hat{D}(\omega) \,|\, n_1l_1\rangle \langle n_1l_1, \varepsilon l \,|\, \hat{U} \,|\, \varepsilon' l', n_1l_1\rangle}{\omega - \varepsilon' + E_{n_1l_1} + i\delta} \right.$$
$$\left. - \frac{\langle n_1l_1 \,|\, \hat{D}(\omega) \,|\, \varepsilon' l'\rangle \langle \varepsilon' l', \varepsilon l \,|\, \hat{U} \,|\, n_1l_1, n_1l_1\rangle}{\omega + \varepsilon' - E_{n_1l_1} - i\delta} \right)_{\delta \to 0}. \qquad (2.2)$$

Here $\langle|\hat{d}|\rangle$ is the dipole matrix element calculated with the Hartree-Fock wave functions (in the r- or the ∇-form), $\langle|\hat{D}(\omega)|\rangle$ is the dipole matrix element with allowance for the intrashell interaction, $E_{n_1l_1}$ is the energy of an electron in the n_1l_1 shell, and $\langle n_1l_1, \varepsilon l|\hat{U}|\varepsilon' l', n_1l_1\rangle$ is the dipole component of the interaction between the electrons of the single shell that undergo the dipole transitions $n_1l_1 \to \varepsilon l$, $\varepsilon' l'$. The latter matrix element is determined by the difference between the direct and exchange Coulomb matrix elements:

$$\langle n_1l_1, \varepsilon l \,|\, \hat{U} \,|\, \varepsilon' l', n_1l_1\rangle = \langle n_1l_1, \varepsilon l \left| \frac{1}{|\mathbf{r} - \mathbf{r}_1|} \right| \varepsilon' l', n_1l_1\rangle$$
$$- \langle n_1l_1, \varepsilon l \left| \frac{1}{|\mathbf{r} - \mathbf{r}_1|} \right| n_1l_1, \varepsilon' l'\rangle. \qquad (2.3)$$

The symbol $(\Sigma, \int)_{\varepsilon', l'}$ in (2.2) denotes summation over all the quantum numbers of the intermediate state (including integration with respect to the energy ε' in the continuous spectrum). For all shells but the s-shells, there are two dipole matrix elements $\langle \varepsilon l \pm 1|\hat{D}(\omega)|nl\rangle$, which determine the partial photoionization cross-sections upon substitution into (2.1) instead of the single-particle amplitudes.

The ARPE method takes account of only part of the residual interaction among the electrons of the given shell. In diagram language one can write Eq. (2.2) in the following form:

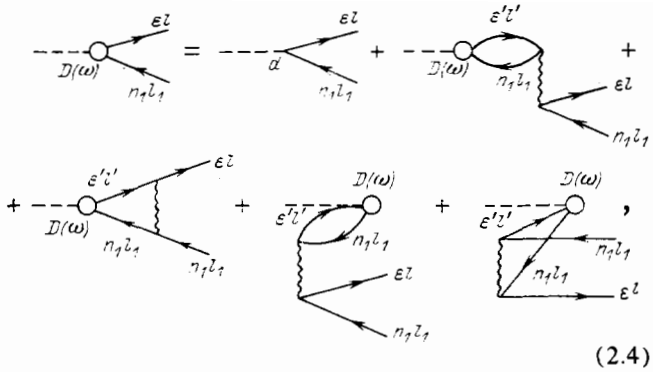

(2.4)

Here a dashed line denotes a quantum of the external field, a line with an arrow to the right (or to the left) indicates a particle, i.e., an electron in the excited state (or a hole, i.e., a core electron of the atom), while a wavy line denotes the interaction $\langle|(1/(\mathbf{r} - \mathbf{r}_1))|\rangle$ between the electrons. Calculations by perturbation theory[8] up to fourth order have shown that precisely the terms of the series of (2.4) yield the main contribution to the amplitude. Physically, within the framework of the ARPE, besides the direct action of the photon on the given electron, one takes account of the small change in the mean self-consistent field arising from absorption of the photon by the other electron shells.

One must take account of the intrashell correlations in describing the total photoionization cross sections, since the latter are determined by the "strong" transitions. Thus, taking account of the intrashell interaction for np^6 and nd^{10} electrons has enabled explaining the behavior of the photoionization cross sections, initially for the noble-gas atoms: Ne, Ar, Kr, and Xe,[7] and then for a number of other atoms.[14,16,26]

For "weak" transitions in the outer and intermediate shells the role of the intrashell correlations is usually small. In these cases henceforth we shall restrict the treatment to presenting the results of only the single-particle Hartree-Fock calculations, while understanding that taking account of the intrashell interaction leads to similar results. However, for "weak" transitions the influence of adjacent shells that possess "strong" transitions proves very significant. Study of the partial photoionization cross sections of shells with "weak" transitions enables one to establish the general features of the intershell interaction.

Let us write the amplitude of the single-electron photoionization of the shell n_1l_1 with transition to the state εl in the form of the two terms:

$$\langle \varepsilon l \,|\, \tilde{\hat{D}}(\omega) \,|\, n_1l_1\rangle = \langle \varepsilon l \,|\, \hat{d} \,|\, n_1l_1\rangle + \langle \varepsilon l \,|\, D^{\kappa}(\omega) \,|\, n_1l_1\rangle. \qquad (2.5)$$

Here the first term describes the direct transition of the electron from the shell owing to absorption of a quantum of the electromagnetic field by one of its electrons. This can be the amplitude obtained in the Hartree-Fock approximation or that obtained with account taken of the intrashell correlations, if they are large. The second term—the intershell correlation amplitude—describes the influence of the other shells of the atom on the ionization of the shell being studied.

In most cases one can restrict the treatment to the first-order perturbation theory in the residual interaction between the electrons belonging to different shells. For simplicity we neglect for now the contribution of the intrashell correlations for a weak transition. In this approximation the

total amplitude of the phototransition $n_1l_1 \to \varepsilon l$ can be written graphically in the form

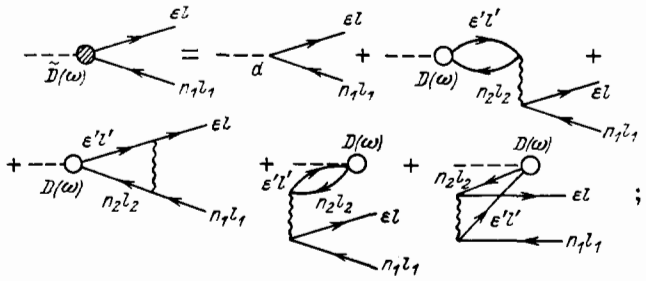

(2.6)

Here each unshaded block corresponds to the amplitude of the $n_2l_2 \to \varepsilon' l'$ transition with allowance for the intrashell correlations determined from (2.4), while a wavy line corresponds to the Coulomb interaction between the electrons of different shells. The four latter terms in (2.6) amount to $\langle|\hat{D}^c(\omega)|\rangle$, the intershell correlation amplitude. It takes account of the process, complex in comparison with that described by the first term in (2.5) and (2.6), of ionization or excitation: the incident γ-quantum is absorbed initially by the n_2l_2 shell ($n_1 \neq n_2$ and $l_1 \neq l_2$) to form a real or virtual intermediate state $n_2l_2 \to \varepsilon' l'$. Then, owing to the interaction between the different shells the quantum energy is transferred to the electrons of the n_1l_1 shell. The analytical expression for the correlation amplitude in the first order in the intershell interaction has the form

$$\langle \varepsilon l \mid \hat{D}^{\text{K}}(\omega) \mid n_1l_1\rangle$$
$$= \sum_{n_2,\, l_2} \left(\sum, \int\right)_{\varepsilon',\, l'} \left(\frac{\langle \varepsilon' l' \mid \hat{D}(\omega) \mid n_2l_2\rangle \langle n_2l_2,\ \varepsilon l \mid \hat{U} \mid \varepsilon' l',\ n_1l_1\rangle}{\omega - \varepsilon' + E_{n_2l_2} + i\delta} - \frac{\langle n_2l_2 \mid \hat{D}(\omega) \mid \varepsilon' l'\rangle \langle \varepsilon' l',\ \varepsilon l \mid \hat{U} \mid n_2l_2,\ n_1l_1\rangle}{\omega + \varepsilon' - E_{n_2l_2} - i\delta} \right)_{\delta \to 0}. \tag{2.7}$$

Here the matrix element for the intershell interaction

$$\langle n_2l_2,\ \varepsilon l \mid \hat{U} \mid \varepsilon' l',\ n_1l_1\rangle \ (n_1 \neq n_2,\ l_1 \neq l_2)$$

is determined, according to (2.3), by the sum of the direct and exchange matrix elements. If we restrict the treatment to taking account of only the one shell n_2l_2, then the summation over n_2 and l_2 in (2.7) is not performed.

As a rule, the matrix elements of the intershell interaction $\langle|\hat{U}|\rangle$ are substantially smaller than the matrix elements defining the interaction among the electrons within a single multielectron shell having a "strong" transition, and they rapidly decline with increasing energy. Therefore, if we restrict the treatment to the first order in the intershell interaction, we can find from Eqs. (2.5)–(2.7) that the influence of the adjacent shells becomes substantial when the following conditions are fulfilled:

1) The dipole matrix element of the transition from the perturbing shell must be large enough

$$|\langle \varepsilon' l' \mid \hat{D}(\omega) \mid n_2l_2\rangle| \gg |\langle \varepsilon l \mid \hat{D}(\omega) \mid n_1l_1\rangle|. \tag{2.8}$$

2) The interacting shells must be close, or at least, of the same order in $E_{n_2l_2} \sim E_{n_1l_1}$, since $\omega = \varepsilon - E_{n_1l_1}$ and the matrix elements have the greatest values at energies of the order of the ionization potential.

These conditions are certainly fulfilled for the outer and intermediate few electron shells when a multielectron shell with a "strong" phototransition proves to lie adjacent.

It is expedient to distinguish the influence of an outer shell on the ionization of a deeper shell and that of an inner shell on an outer shell. Owing to the differing manifestation of the intershell interaction for these cases, we shall examine them separately. We note also that Eqs. (2.2)–(2.7) have been written for atoms with filled shells, since they are the simplest and most convenient objects for theoretical study.

2.2. Influence of the inner shells

Let us examine the influence of the inner shells on the photoionization of electrons from the outer shells. In this case we can arbitrarily distinguish several regions of differing manifestation of the intershell correlation:

1) up to the ionization threshold of the inner shell, in which only the virtual excitations of its electrons exert an influence on the ionization;

2) at energies larger than its ionization potential (interaction of open channels);

3) the region of energies in the vicinity of discrete excitations of the inner shell, which is manifested in the absorption spectrum in the form of a set of autoionization resonances.

In this section we shall limit the discussion to a qualitative treatment of the first two regions.

The radius r_1 of the outer shell is usually considerably greater than the radius r_2 of the inner shell, while the ionization potential is much smaller. Hence the expressions (2.5)–(2.7) for the photoionization amplitude are simplified. If the difference between the ionization potentials of the outer and inner shells is large, then we can neglect the exchange interaction in $\langle|\hat{U}|\rangle$, while the dipole component of the Coulomb matrix element for $r_1 \gg r_2$ is simplified:

$$\left\langle n_2l_2,\ \varepsilon l \left| \frac{1}{|\mathbf{r}_1 - \mathbf{r}_0|} \right| \varepsilon' l',\ n_1l_1 \right\rangle \approx \langle n_2l_2 \mid \mathbf{r}_2 \mid \varepsilon' l'\rangle \left\langle \varepsilon l \left| \frac{\mathbf{r}_1}{r_1^3} \right| n_1l_1 \right\rangle. \tag{2.9}$$

Upon substituting (2.9) into the correlation amplitude of (2.7), we can write the total photoionization amplitude (2.6) in the following form (in the form involving the distance $\hat{d} = \mathbf{r}$):

$$\langle \varepsilon l \mid \hat{\tilde{D}}(\omega) \mid n_1l_1\rangle \approx \langle \varepsilon l \mid \mathbf{r}_1 - \frac{\mathbf{r}_1}{r_1^3}\alpha(\omega) \mid n_1l_1\rangle, \tag{2.10}$$

Here $\alpha(\omega)$ is the dynamic dipole polarizability of the inner shells of the atom, as determined by the relationship[16]

$$\alpha(\omega) = 2\left(\sum, \int\right)_{\varepsilon',\, l'} \frac{\langle \varepsilon' l' \mid \hat{D}(\omega) \mid n_2l_2\rangle \langle n_2l_2 \mid \mathbf{r}_2 \mid \varepsilon' l'\rangle}{(\varepsilon' - E_{n_2l_2})^2 - \omega^2} (\varepsilon' - E_{n_2l_2}). \tag{2.11}$$

At low energies ω up to the ionization threshold of the shell n_2l_2, we can neglect the frequency-dependence $\alpha(\omega)$, and retain the static polarizability $\alpha = \alpha(0)$ in (2.10):

$$\langle \varepsilon l \mid \hat{\tilde{D}} \mid n_1l_1\rangle \approx \left\langle \varepsilon l \left| \mathbf{r}_1 - \frac{\alpha}{r_1^3}\mathbf{r}_1 \right| n_1l_1 \right\rangle. \tag{2.12}$$

The dipole matrix element was first presented in this form in Ref. 27, and has been employed for eliminating the discrepancy between the theoretical and experimental data involving the sums of the oscillator strengths in the alkali metals

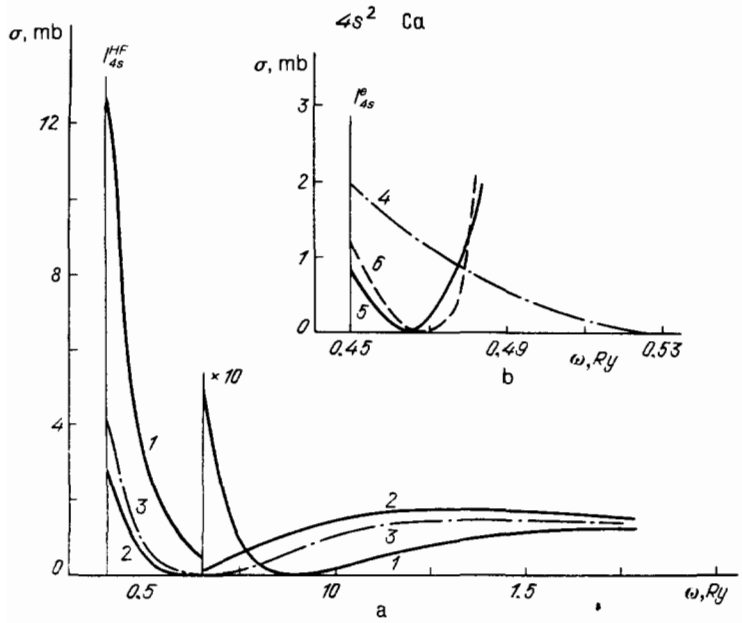

FIG. 1. Photoionization cross section of the $4s^2$ shell of Ca. Calculated: *1, 2*—Hartree-Fock approximation, σ_0^r and σ_0^∇ respectively; *3*—ARPE with allowance for intrashell correlations; *4*—with allowance for the influence of the $3p^6$ shell[13]; *5*—with allowance for the influence of the $3p^6$ shell and two-electron resonances.[32] Experiment[29]—curve *6*. I^{HF} and I^e are the theoretical and experimental ionization thresholds.

(see Sec. 3.2 for more details on the photoionization of alkali atoms). Since these atoms contain one *s* electron each in the outer shells, intrashell correlations are completely lacking for them.

However, to describe the dependence of the photoionization cross section on ω, taking account of the static polarizability is evidently insufficient, even for *n*s shells of the alkali-metal atoms, not to mention filled shells, since the interaction among shells is highly dependent on the energy. Moreover, for many atoms the radius of the inner shell where the dynamic polarizability substantially affects the removal of the outer electron is of the same order of magnitude as that of the outer shell. Therefore, Eqs. (2.10)–(2.12) can be employed only for qualitative estimates of the amplitudes.

A striking example of the influence of an inner shell up to its ionization threshold is given by the behavior of the photoionization cross section of the outer ns^2 shells in the atoms of the alkaline-earth metals. They obey the condition (2.8): the $(n-1)p^6$ or $(n-1)d^{10}$ shells closest in energy to the *n*s electrons have strong transitions to the discrete and continuous spectra.[16,18,28]

Figure 1 presents the results of different calculations of the photoionization cross sections of the $4s^2$ shell of Ca and the experimental data[29] up to the ionization threshold of the $3p^6$ shell. The cross sections obtained in the single-electron Hartree-Fock approximation in the "*r*" and "∇" forms (σ_0^r and σ_0^∇) strongly differ from the experimental values and from each other. For the two 4s electrons the intrashell interaction also proves substantial: taking it into account brings σ^r and σ^∇ closer together, but at the same time the discrepancy with experiment remains large.[13] The perturbation of the inner $3p^6$ shell, which mainly is governed by the dipole transitions $3p \to 3d$, εd to a discrete level and to the continuous spectrum has diminished the cross section at the $4s^2$ threshold twofold. Taking account of this influence in different calculations[13,30] has improved the agreement with experiment, yet has not yielded final agreement. As recent experimental[31] and theoretical[32,33] studies have shown, discrete two-electron excitations in the $4s^2$ shell itself, in addition to the intershell interaction, play a large role in the formation of the photoabsorption spectrum of $4s^2$Ca. The former, especially the transition $4s^2 \to 3d5p$, have a relatively large oscillator strength and lie in the immediate vicinity of the single-ionization threshold of $4s^2$. These excitations have been taken into account by a method lying outside the framework of the ARPE and using the MPT.[32] It was shown that the two-electron excitations diminish the single-photoionization cross section at the threshold by interfering with the continuous spectrum of the transition $4s \to \varepsilon p$ (see Fig. 1b).

At large energies up to the ionization threshold of the $3p^6$ shell, autoionization resonances involving excitation of the 3p electrons dominate in the photoabsorption spectrum of Ca.[32,33]

In Zn atoms the 3d electrons exert the major influence on the photoionization cross section of the outer $4s^2$ shell.[16,18] The behavior of the cross section near the 4s threshold is analogous in general features to σ_{4s} in Ca. We note only that in Zn both dipole transitions from the inner shell $3d \to \varepsilon f$ and $3d \to \varepsilon p$ have about the same effect on the 4s electrons. This involves the fact that, although the $3d \to \varepsilon f$ transition is the principal one, the maximum of its cross section is shifted into the region of large energies as compared with $3d \to \varepsilon p$, where the maximum occurs at the threshold region. Moreover, the $3d \to mp$ ($m = 4, 5, \ldots$) transitions have relatively large oscillator strengths. Taking account of these transitions diminishes the cross section σ_{4s} in the threshold region of the $4s^2$ shell and gives rise to a resonance structure at large energies.[18,34]

In the heavier alkaline-earth elements, such as Cd, Ba, and Hg, the situation for the outer ns^2 shells proves similar to that found in Ca and Zn: the photoionization cross section σ_{ns} is governed by the intershell interaction and by the influence of the virtual excitations of the inner shell.[28,35–37] For the lighter elements Be and Mg the intershell interaction is considerably weaker and does not affect the photoionization process so substantially.[38–40]

Beyond the ionization threshold of the inner shell, its

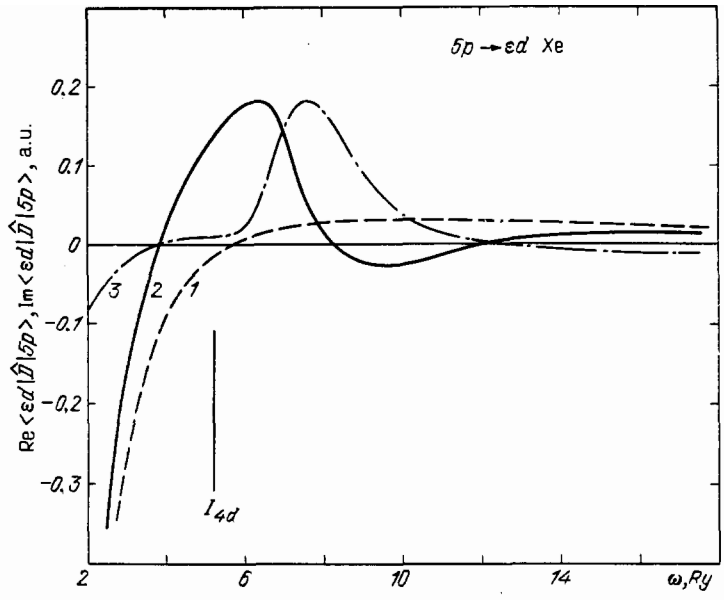

FIG. 2. The amplitude of the $5p \to \varepsilon d$ transition in Xe in the vicinity of the ionization threshold of the $4d^{10}$ shell.[41] *1*, *2*—$\mathrm{Re}\langle \varepsilon d|\hat{D}|sp\rangle$, respectively without and with allowance for the influence of the $4d^{10}$ shell; *3*—$\mathrm{Im}\langle \varepsilon d|\hat{D}|sp\rangle$ with allowance for the influence of the $4d^{10}$ shell (without allowing for it $\mathrm{Im}\langle|\hat{D}|\rangle$ is very small, $\sim 10^{-3}$–10^{-4} a.u.).

influence is determined not so much by the integral oscillator strength as by the concrete dependence of its cross section on the energy. The sharper the energy dependence of σ_{inner} is, the stronger its influence on the outer electrons proves to be, as is usually manifested in the form of a maximum in the photoionization cross section of the latter. As a rule, this maximum qualitatively copies the ionization cross section of the inner shell.

We can conveniently illustrate what we have said with the example of photoionization of the $5p^6$ shell of Xe (and the elements following it in the periodic system) in the vicinity of and above the ionization threshold of the $4d^{10}$ shell. At quantum energies $\omega > I_{4d}$ the contribution of the 4d electrons dominates the total photoabsorption cross section. Here, while in Xe the maximum of the cross section lies at energies ~ 30 eV beyond the threshold,[4,16] with increasing charge Z of the nucleus, the maximum becomes higher and approaches the threshold, yet does not emerge into the discrete spectrum, as is manifested in the large oscillator strength of the $4d \to 4f$ transition. Thus one can systematically trace the influence of the form of the ionization cross section of the inner $4d^{10}$ shell on the ionization of the 5p electrons with increasing Z.

One cannot restrict the treatment to a simple estimate of the correlation amplitude (2.7) in this case. However, one can see an important circumstance from (2.7): at energies above the ionization threshold $\omega + E_{n_2 l_2} > 0$, the real part of the amplitude in (2.7) changes sign. The imaginary part of the amplitude is proportional to the product:

$$\mathrm{Im}\,\langle \varepsilon l \mid \hat{D}^{*}(\omega) \mid n_1 l_1\rangle$$

$$\sim \langle \varepsilon' l' \mid \hat{D}(\omega) \mid n_2 l_2\rangle \langle n_2 l_2, \varepsilon l \mid \hat{U} \mid \varepsilon' l', n_1 l_1\rangle, \qquad (2.13)$$

and can also vary strongly with the energy. Figure 2 shows the real and imaginary parts of the amplitude for the $5p \to \varepsilon d$ transition in Xe, as obtained within the framework of the ARPE without and with allowance for the effect of the $4d^{10}$ electrons, respectively.[41] We see that the action of the $4d^{10}$ shell has led to a very complicated dependence on ω. The $4d^{10}$ shell affects the amplitude of the $5p \to \varepsilon s$ transition considerably more weakly.

In the partial photoionization cross section of the $5p^6$

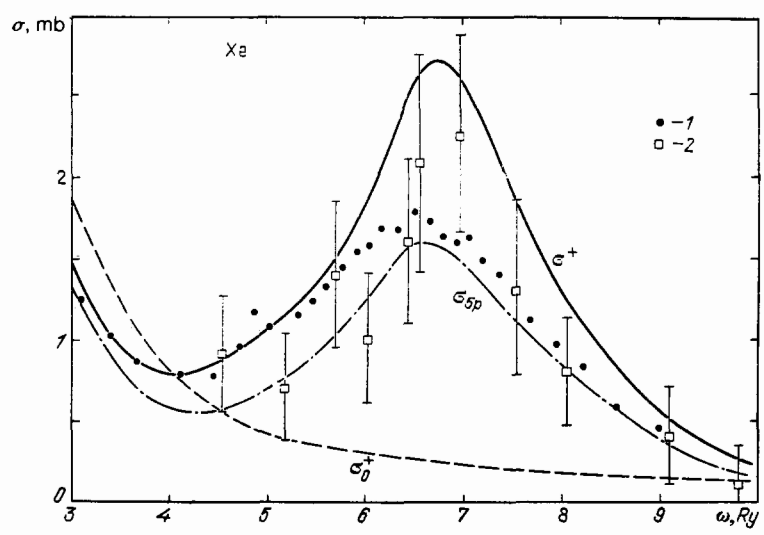

FIG. 3. Cross section for single photoionization σ_0^+ without allowance for the influence of the $4d^{10}$ shell and σ^+ with allowance for its influence and the partial contribution of the $5p^6$ shell σ_{5p} of Xe in the vicinity of the threshold of the $4d^{10}$ shell. Experiment for σ^+: *1*—Ref. 42; *2*—Ref. 43.

shell of Xe including the $5p \to \varepsilon d$ and $5p \to \varepsilon s$ transitions (Fig. 3), the amplitude variations have been smoothed out, so that the influence of the $4d^{10}$ shell is expressed in the appearance of only one maximum in the cross section.[13,41] We note that here we are dealing with the interaction of two multielectron shells having "strong" dipole transitions to the continuous spectrum, but in substantially different energy regions: σ_{5p} gives the fundamental contribution to the overall cross section up to $\omega \lesssim 50$ eV, while σ_{4d} contributes beginning at $\omega \gtrsim 70$ eV.[4,16] In the vicinity of the threshold the $4d^{10}$ transitions from the $5p^6$ shell become weak, and then become more subject to the influence from the other transitions.

A substantial effect of an inner shell above its threshold on an outer shell is manifested in the increase in the cross section σ^+ for yield of singly-charged ions in a number of atoms. Thus, for example, in the Xe atom the increase in the yield of Xe^{+1} ions when $\omega > I_{4d}$ can involve only the ionization of the outer $5s^2$ and $5p^6$ shells, since the ionization of the inner 4d electrons leads to formation of doubly charged ions (owing to the overwhelming probability of Auger decay of a 4d vacancy as compared with radiative decay). The cross section σ^+ is composed of the cross sections for removal of electrons from the $5p^6$ and $5s^2$ shells. The curve σ^+ for the yield of singly charged ions has a maximum beyond the threshold I_{4d} that is fully due to the influence of the $4d^{10}$ shell,[16] as is illustrated in Fig. 3. The experimental data[42,43] confirm the great role of the intershell interaction.

The $3d^{10}$ electrons of Kr exert an analogous effect on the ionization of the outer $4p^6$ and $4s^2$ shells.[16,42] However, it is expressed considerably more weakly than in Xe, which involves the relatively small amplitude of the $3d \to \varepsilon f$ transition and its smoother energy dependence.

In the atoms following Xe in the periodic table (Cs, Ba, La), the effect of the $4d^{10}$ shell on the photoionization of the outer electrons is manifested even more strongly than in Xe[44–46] (see Sec. 5.1). With further increase in the nuclear charge Z it is manifested mainly in the form of an autoionization resonance involving the $4d \to 4f$ transition.[47]

Thus, in the vicinity of its threshold the considerable influence of an inner shell having a strong transition to the continuous spectrum has a quasiresonance character and is typical of most heavy atoms. Qualitatively we can represent the pattern of the photoionization process as follows. The incident electromagnetic field gives rise to oscillations of the electrons of the inner shell with great amplitude. Owing to the strong coupling with the outer electrons, these oscillations transfer to the latter the energy of the absorbed quantum and thus enhance their ionization probability. Thus the phenomenon recalls autoionization resonances in its nature. However, in the cases being studied, we are not dealing with the interference of a discrete level with the continuous spectrum, but that of an energy-localized maximum of the continuous spectrum of one shell with the diffuse continuous spectrum of another shell.

2.3. Influence of the outer shells

The outer multielectron shells can substantially screen the electrons internal to them from an external electromagnetic field. When the coupling between the shells is strong enough, also the ionization of the inner shells can be amplified. This effect in the behavior of the partial photoionization cross sections of the outer ns^2 shells of atoms of the noble gases was first predicted theoretically,[12,13] and then found experimentally.[48–50] It turned out that the probability of ionization of the ns^2 electrons is governed over a broad energy range by the influence of the outer np^6 shells.

In contrast to the case treated in Sec. 2.2, here we are always dealing with the interaction of two open channels in the photoionization process. An overall estimate of the magnitude of the intershell correlation amplitude of (2.7) is difficult, and one can perform it only by using concrete models for calculating the Coulomb and dipole matrix elements. The calculations show that, in the most important energy region, the correlation amplitude has a fixed sign and declines rapidly with increasing ω.

The fact that the intershell interaction is substantial for the outer shells of the atoms of the noble gases is also implied by the fulfillment of the conditions (2.8). In fact, the contribution of the ns^2 shells to the overall photoionization cross section amounts to 1–3%, while the main contribution at quantum energies up to 80–100 eV comes from the $np \to \varepsilon d$ dipole transition from the np^6 shell.[4,7] The difference in ionization thresholds of the ns^2 and np^6 shells for all noble-gas atoms is relatively small and amounts to $\sim$ 10–15 eV. Consequently the intershell correlation amplitude of (2.7), where the $np \to \varepsilon d$ transition has been taken into account in the intermediate state $(n_2 l_2 \to \varepsilon' l')$, becomes of the same order of magnitude as the amplitude of the direct $ns \to \varepsilon p^2$ transition from the ns^2 shell. Thus, for the Ar atom the correlation amplitude describing the overall influence of the $3p \to \varepsilon d$ and $3p \to \varepsilon s$ transitions exceeds the amplitude of the direct $3s \to \varepsilon p$ transition in absolute magnitude even severalfold at the ionization threshold of the $3s^2$ shell, and has an opposite sign. With increasing ω, the matrix element $\langle \varepsilon p | \hat{D}^k | 3s \rangle$ declines rapidly, so that, starting at a certain energy, the direct amplitude becomes greater than the correlation amplitude. Consequently the real part of the amplitude passes through zero, and as it turns out, the imaginary part also vanishes near this energy. Hence a minimum appears in the photoionization cross section, which is absent when one neglects the effect of the $3p^6$ electrons. We can see in Fig. 4, which shows the cross sections of the $3s^2$ shell of Ar in both approximations, the role of the intershell interaction, which has led not only to quantitative, but also to qualitative changes. The experiments of several groups[48,49,51,52] and the calculations within the framework of other methods[9,53–55] have confirmed this result for σ_{3s} in Ar.

The physical explanation of such behavior of the photoionization cross section is as follows. The multielectron outer $3p^6$ shell screens the deeper $3s^2$ shell from the external electromagnetic field, with a degree of screening depending on the frequency of the incident light. At low energies close to the ionization threshold of the $3s^2$ shell, the incident electromagnetic wave is absorbed mainly by the $3p^6$ shell, "pumps" it, and removes the 3s electrons, owing to the strong coupling with $3s^2$. At the ionization threshold $\omega \gtrsim I_{3s}$ actually the entire process is governed by the influence of the 3p electrons on the 3s. With increasing energy of the quanta, the dipole polarizability of the $3p^6$ shell declines and the mutual coupling between the shells decreases. At a certain photon frequency at which the forced displacements of the s electrons owing to direct absorption by them of a photon and

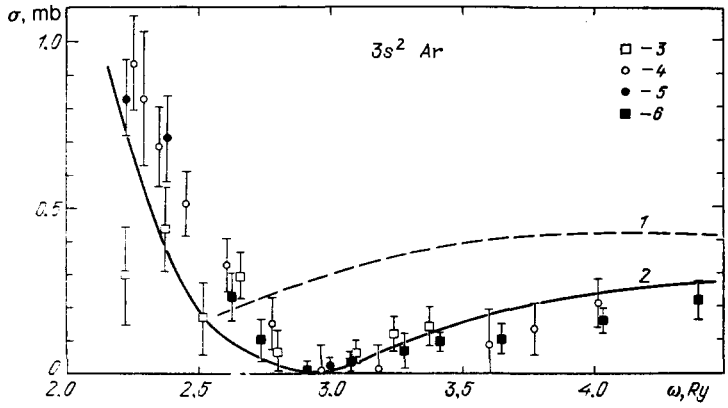

FIG. 4. Photoionization cross section of the $3s^2$ shell of Ar *1*—ARPE within the framework of the $3s \to \varepsilon p$ transition, *2*—ARPE with allowance for the influence of the $3p^6$ electrons.[13] Experiment: *3*— Ref. 48, *4*—Ref. 51, *5*—Ref. 49, *6*—Ref. 52.

the displacement under the action of the p electrons occur in counterphase, the ionization cross section has a minimum value. Upon further energy increase, the outer shell becomes ever more "transparent" to the incident light and the photoionization cross section approaches a value determined by the direct interaction of the radiation with the 3s electrons.

An analogous behavior of the partial photoionization cross section of the outer s electrons has been found theoretically[13] and experimentally[49] in the atoms Kr and Ne (Fig. 5). For the Ne atom the intershell interaction is weaker and the amplitude of the $2p \to \varepsilon d$ transition is smaller than for the corresponding transitions in the other noble-gas atoms. Hence the screening influence of $2p^6$ is smaller and a minimum in the cross section does not appear.[9,13,50,55]

A strong influence of the outer shells on the deeper shells is characteristic not only of strong outer shells. As concrete calculations[16,37] for Pd, Xe, Cs, Ba, and Hg have shown, in heavy atoms the intermediate $4d^{10}$ and $5d^{10}$ shells always strongly screen the lower-lying p^6 and s^2 shells.

2.4. Collectivization of ns^2 shells

In heavy atoms in which the main contribution to the total photoionization cross section comes jointly from several multielectron shells, the situation often arises in which they all exert a strong influence on the ionization of the few electron shells. In this case the correlation amplitude entering into (2.5) is presented in perturbation theory first-order in the intershell interaction in the form of the summation:

$$\langle \varepsilon l \mid \hat{D}^{\kappa}(\omega) \mid n_1 l_1 \rangle = \sum_i \langle \varepsilon l \mid \hat{D}^{\kappa}_{(n_i l_i)}(\omega) \mid n_1 l_1 \rangle. \qquad (2.14)$$

Here every term is determined by Eq. (2.7) and describes the influence of the shell $n_i l_i$ on the amplitude of the transition from $n_1 l_1$. Since the direct and correlation amplitudes generally have a different dependence on the quantum energy and can change sign at certain ω values, the total amplitude determined by their sum can be a very capricious function of the energy.

This is illustrated strikingly by the example of photoionization of the $5s^2$ shell of I, Xe, Cs, Ba, and the atoms of the rare-earth elements. In all of them the 5s electrons lie in energy between the two multielectron shells $5p^6$ and $4d^{10}$, which possess strong dipole transitions. Figure 6 shows the results of calculations of the photoionization cross section of the $5s^2$ shell of Xe in different approximations[16,57] and the experimental data.[43,49,58] Upon allowing for the influence of the adjacent shells, the smooth behavior of the cross-section in the Hartree-Fock approximation typical of all outer ns^2 shells of noble-gas atoms is replaced by strong variations in magnitude over a broad energy range (curve *3* in Fig. 6). We note that the influence of the deeper $4d^{10}$ shell is large even at the threshold of the $4d^{10}$ shell itself (curve *2* in Fig. 6). The region of the influence of the electrons of the $5p^6$ shell extends just as far. Thus the photoionization cross section of

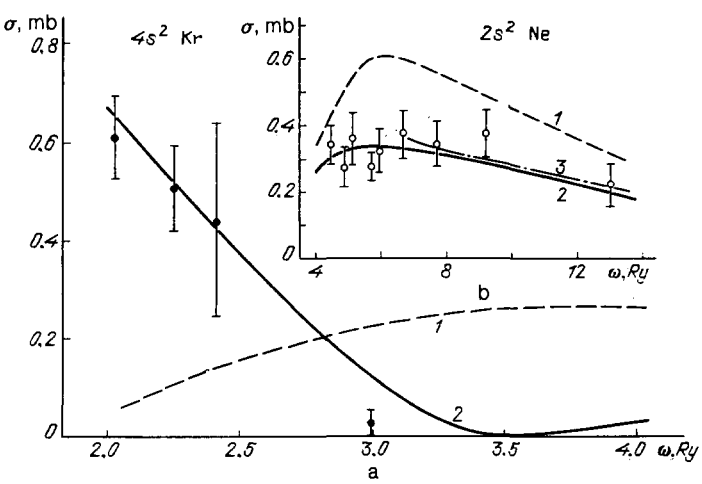

FIG. 5. Photoionization cross section of the $4s^2$ shell of Kr (a) and the $2s^2$ shell of Ne (b). ARPE calculation[13]: *1*—direct ionization of s electrons; *2*—with allowance for the influence of the outer p electrons. Experiment for Ne: curve *3* from Ref. 50, ○ from Ref. 56, ● from Ref. 49.

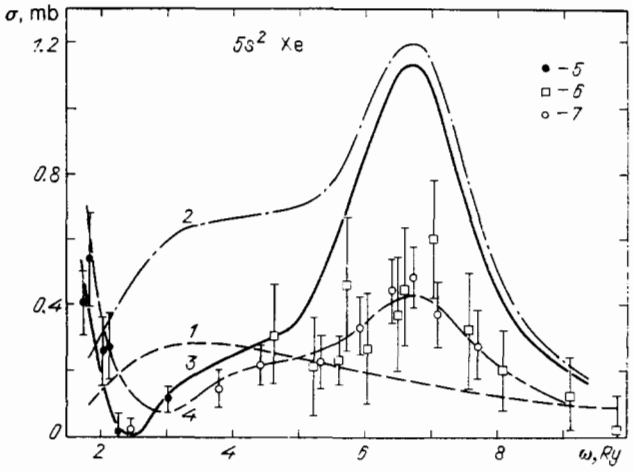

FIG. 6. Photoionization cross section of the $5s^2$ shell of Xe. Calculation: *1*—Hartree-Fock approximation; *2*—ARPE wth allowance for the influence of the $4d^{10}$ shell; *3*—ARPE with allowance for the $5p^6$ and $4d^{10}$ shells[16,57]; *4*—with allowance for the intershell interaction and the spectroscopic factor of the $5s^2$ shell.[57,62] Experiment: *5*—Ref. 49, *6*—Ref. 43, *7*—Ref. 58.

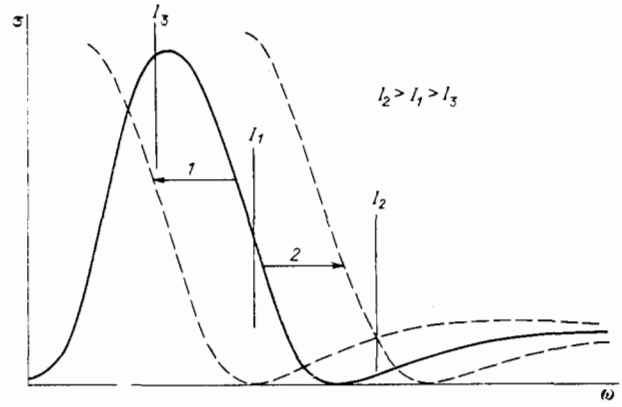

FIG. 7. Generalized curve of the dependence of the partial photoionization cross section of an s^2 shell on the photon energy. I_{1-3} are the ionization potentials of this shell in different atoms. The arrows indicate the shift of the curve upon allowing for the intershell interaction: *1*—from an inner shell; *2*—from an outer shell.

the 5s electrons in Xe is governed by the simultaneous interaction of all three shells: $5p^6$, $5s^2$, and $4d^{10}$, as is confirmed by the experimental measurements[43,49,52,58–60] and other calculations[25,61,62] (we shall discuss curve *4* in Fig. 6 in Sec. 5.3).

Since the photoionization cross section of the $5s^2$ shell has fully lost the features of individual behavior (curve *1* in Fig. 6), it is pertinent to speak of the collectivization of the 5s electrons under the influence of the surrounding multielectron shells. Such a collectivization is characteristic of the $5s^2$ shells of many elements, beginning with Cd ($Z = 48$).[28] However, the dependence of the photoionization cross section σ_{5s} on the energy undergoes successive changes with increasing nuclear charge Z. Thus, on going from Xe to La the minimum in σ_{5s} shifts into the region of the discrete spectrum.[16]

By analyzing the results of the different calculations and comparing them with experiment, we can draw a number of qualitative conclusions on the behavior of the partial photoionization cross sections of neutral isolated atoms, on their dependence on the nuclear charge, and on the influence of the intershell interaction. Let us demonstrate them with the example of the ns^2 shells of atoms, although they also pertain to a considerable degree to the other shells.

The photoionization cross sections for the ns^2 shells for different atoms and values of n (= 1, 2, 3, . . .) can be described qualitatively by different regions of a single universal curve having maxima and a minimum (Fig. 7). These regions are determined by the position of the ionization threshold of the shell being studied with respect to the curve, while retaining the part of the cross section lying at large photon energies and truncating it at small energies (see Fig. 7). A direct calculation of the cross sections in the Hartree-Fock approximation and with allowance for multielectron correlations confirms this qualitative picture. Thus, in the atoms of the alkali and alkaline-earth metals, the ionization potential I_{ns} of the outer shell is small, the cross section has a minimum, and hence the curve is "truncated" in Fig. 7 in the vicinity of I_1 (see σ_{4s} in Ca in Fig. 1). With increasing Z, the ns electrons cease to be outer electrons, the ionization potentials increase, and gradually shift into the region of large ω. Thus, in the noble-gas atoms the photoionization cross section of the ns^2 shells in the Hartree-Fock approximation is governed by a part of the curve that starts beyond the minimum ($I_{ns} \sim I_2$; see Fig. 5, σ_{4s} in Kr—curve *1*).

One can say the same about the p^6 and d^{10} shells. The cross sections of the outer np^6 shells in the atoms of the noble gases have a powerful maximum at the ionization threshold and a minimum following it. That is, they are also governed by the curve of Fig. 7 starting at I_3. In the deeper p shells the maximum at the threshold declines, and the minimum shifts closer to the threshold and then emerges into the region of the discrete spectrum.

The intrashell correlations are capable of substantially altering the magnitude of the photoionization cross section, but they usually do not lead to qualitative changes in it as a function of the energy. Yet, conversely, the intershell interaction often leads to qualitative changes that can be represented as follows within the framework of the proposed scheme. The influence of the inner shell "shifts" the cross section curve of the shell being studied toward lower energies with respect to its ionization potential (case *1* in Fig. 7). If the cross section had a maximum at the threshold, then when we take account of the interaction with the inner shell, its magnitude declines, while the minimum approaches the threshold or completely emerges into the discrete spectrum. The cross section increases beyond the minimum, while in the vicinity of the ionization potential of the perturbing shell it can generally have a resonance character (see Figs. 1, 3, and 6).

The influence of the outer shells opposes that of the inner shells, and leads to "repulsion" of the cross section curve into the higher-energy region (case *2* in Fig. 7). This is precisely the situation in the noble-gas atoms, in which a minimum appears in the photoionization cross section upon taking account of the influence of the np^6 shells that was lacking in the single-particle calculation, or more exactly, lay in the prethreshold region (see Figs. 4–6).

Analogously the ionization threshold I can shift instead of the cross section curve shifting.

The shift of the photoionization cross section under the influence of the surrounding shells affects mainly the ns^2

shells as being the most subject to their action. Of course, it cannot be understood as a parallel displacement of the curve $\sigma(\omega)$ with respect to the energy. Owing to the dependence of the intershell interaction on ω, this displacement occurs only in a certain restricted region of quantum energies, and its magnitude differs for different values of ω. Of course, the described simple pattern is crude. Yet it enables one to predict qualitatively the behavior of the cross sections of different shells with changing nuclear charge of the atom and the effect of the intershell interaction in the variation of the dependence of σ on the energy of the quantum .

2.5. Ionization by fast particles

Studying the ionization of atoms by fast electrons (or other particles) makes it possible to trace the dependence of the intershell interaction on the momenta q transferred in scattering and the angular momenta λ. Besides dipole transitions, the transfer to an atom of different angular momenta λ leads likewise to monopole, quadrupole, and also other transitions in the atom. Thus it enables elucidating the role of the components of the intershell interaction of varying multipole character.

The differential inelastic-scattering cross section for fast electrons is proportional to the density of generalized oscillator strengths (GOS) $\partial f(\omega, q)/\partial\omega$, and can be written in the form[63]

$$\frac{d^2\sigma}{d\omega\, d\Omega} = \frac{4\pi}{\omega E}\frac{\partial f(\omega, q)}{\partial\omega}\frac{d\ln q^2}{d\Omega}. \tag{2.15}$$

Here E is the energy of the incident electron, ω and q are the energy and momentum transferred to the atom during scattering, and $d\Omega = 2\pi \sin\theta\, d\theta$ is the element of solid angle into which the incident electron is scattered. The generalized oscillator strengths of a single-particle transition from the initial state i to the final state m are determined by the expression (in the "r" or "distance" form)[16,63]:

$$\frac{\partial f^{r}_{mi}(\omega, q)}{\partial\omega} = \frac{\omega}{q^2}\,|\langle m\,|\exp(i\mathbf{qr})\,|\,i\rangle|^2. \tag{2.16}$$

Upon expanding $e^{i\mathbf{q}\cdot\mathbf{r}}$ in Legendre polynomials, we obtain the partial GOS densities pertaining to the particular component corresponding to the angular momentum of the interaction λ:

$$\frac{\partial f^{r(\lambda)}_{mi}(\omega, q)}{\partial\omega} = \frac{N_i(E_m - E_i)}{q^2}\left|\left\langle m\left\|\frac{\partial f^{r}_{\lambda}}{\partial\omega}\right\|i\right\rangle\right|^2. \tag{2.17}$$

Here N_i is the number of electrons in the ith state. In the one-electron approximation, the reduced matrix element entering into (2.17) is written in the following form ($i = nl$, $m = n'l'$):

$$\left\langle n'l'\left\|\frac{\partial f^{r}_{\lambda}}{\partial\omega}\right\|nl\right\rangle = [(2l+1)(2l'+1)]^{1/2}\begin{pmatrix} l & \lambda & l' \\ 0 & 0 & 0\end{pmatrix}^2\int_0^\infty P_{n'l'}(r)\,P_{nl}(r)\,j_\lambda(qr)\,dr. \tag{2.18}$$

Here $P_{n'l'}(r)$ and $P_{nl}(r)$ are the radial components of the one-electron wave functions of the electron in the initial and final states, and $j_\lambda(qr)$ is the spherical Bessel function of order λ. When $q \to 0$ and $\lambda = 1$, we obtain the reduced matrix elements of the photoeffect, which can also be introduced into Eqs. (2.1) and (2.2) on separating the angular parts of the wave functions. Analogously one can define the GOS density in terms of an operator written in the "velocity" form.[16,63]

In taking account of the multielectron correlations, instead of the reduced matrix element of (2.18) that enters into (2.17), one substitutes the corresponding matrix element defined by expressions analogous to those written for the dipole component in (2.2)–(2.6).

In the limiting case of a transferred momentum $q \to 0$, only the dipole component of the interaction "survives." Therefore, in ionization by fast electrons the influence of the intershell correlations is manifested in a way analogous to that in the photoionization process.

Let us trace the variation of the intershell interaction with increasing q initially with the example of the dipole component of the GOS density.

With increasing q, the influence of the outer shells on the ionization of the deeper shells declines. The reason for this is that the incident electron penetrates ever more deeply into the atom with increasing q. Here the effective range r_e of the interaction with it finally becomes smaller than the radius of the outer shell. The outer electrons screen the inner shell to an ever smaller extent from the action of the incident electron.[64] Figure 8 shows the dipole component of the GOS density for the $3s^2$ shell of Ar as a function of the energy of the ejected electron for two values of q (for $q \to 0$, see Fig. 4). The curve of the GOS density undergoes substantial variations with q, and already at $q = 1.85$ at. units the influence of the outer $3p^6$ shell is small.

On the contrary, the influence of the inner shells on the ionization of electrons from the outer shells can remain substantial even at rather large values of transferred momenta q. Moreover, since the rate of decline of the ionization amplitude is determined by the product qr_e, while the radius of the inner shell is smaller than that of the outer, the contribution of the direct amplitude that enters into (2.5) declines more rapidly with increasing q than the correlation amplitude. Thus the relative role of the inner electrons can increase. This is demonstrated by the dependence of the GOS density of the $5s^2$ shell of Xe on the momentum q (Fig. 9)[64] with allowances for the influence of the $5p^6$ and $4d^{10}$ shells. As

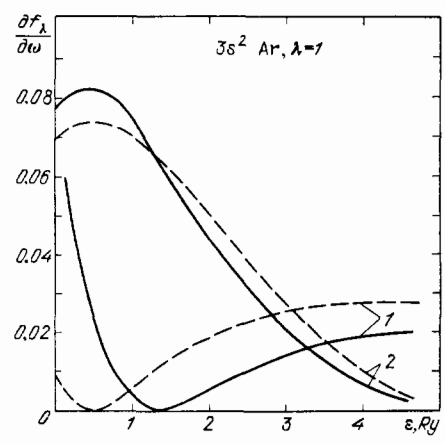

FIG. 8. Dipole component of the GOS density of the $3s^2$ shell of Ar. *1*—$q = 0.65$ a.u.; *2*—$q = 1.85$ a.u. Dotted line—with allowance only for the influence inside the $3s^2$ shell; solid lines—with allowance for the influence of the $3p^6$ shell.[64]

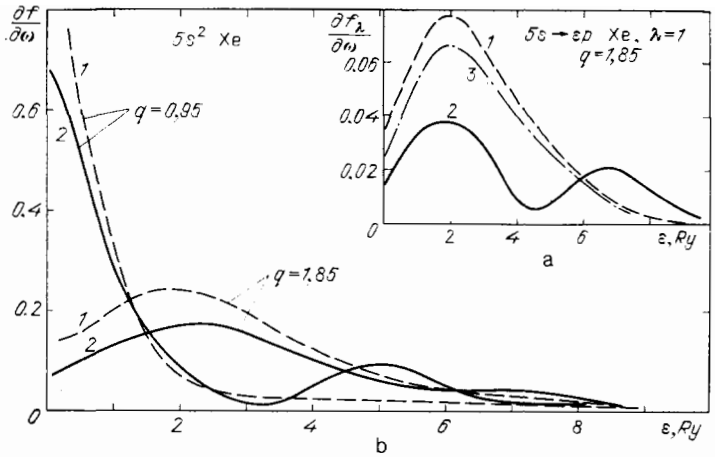

FIG. 9. Dipole component of the GOS density for a transferred momentum $q = 1.85$ a.u. (a) and the total GOS density for $q = 0.95$ and 1.85 a.u. (b) for the $5s^2$ shell of Xe. *1*—direct amplitude; *2*—with allowance for the influence of the $5p^6$ and $4d^{10}$ shells[62]; *3*—with allowance for the influence of only the $5p^6$ shell.

$q \to 0$, the dipole component of the GOS density as a function of the energy of the ejected electron behaves like the photoionization cross section (see Fig. 6) of the $5s^2$ shell. With increasing q a minimum arises in the GOS density, even in the zero-order approximation (with account taken of the intrashell correlations). Therefore the influence of the $5p^6$ and $4d^{10}$ shells gives rise to an increase in the GOS density before and after the minimum, and shifts it, while as a whole the GOS curve remains similar to that for small q. When $q > 1$ the influence of the outer $5p^6$ shell declines sharply, whereas allowing for the action of the deeper $4d^{10}$ shell gives rise to strong qualitative and quantitative changes (see Fig. 9a).

For the components of the GOS density of other multipole types, the intershell interaction is not manifested so sharply. Taking account of it does not lead to a qualitative change in the behavior of $\partial f/\partial\omega$ for all q. However, the numerical changes can be significant. Thus, for monopole transitions the influence of the outer $3p^6$ shell in Ar reduces the partial GOS density of the 3s electrons by 10–40% in the vicinity of the ionization threshold up to $q \sim 2$ at. units.[64] About the same pattern is found when one takes account of the inner shells (e.g., the influence of $4d^{10}$ on the ionization of $5s^2$ in Xe[64]). For quadrupole transitions and those of higher multiple type, the influence of the intershell interaction is considerably weaker. The differential cross section in (2.15) is proportional to the GOS density of (2.16). For small transferred momenta, it is governed by the contribution of the dipole component. Therefore the scattering cross section for fast electrons with ionization of the outer s electrons is collective in character, just as in the photoionization process. With increasing momentum transfer q, the contribution rises of monopole and especially of quadrupole transitions, for which the effect of the surrounding shells is smaller than for the dipole transitions. Therefore the manifestation of the intershell interaction in the differential ionization cross sections by fast electrons, even of shells of small ionization cross section, becomes smaller with greater q. The total GOS density for the $5s^2$ shell of Xe for $q = 0.95$ at. unit (see Fig. 9b) generally resembles the photoionization cross section and the GOS density for small q. However, at $q = 0.95$ the maximum at the ionization threshold is not due to the influence of the outer $5p^6$ shell, but arises mainly from the contribution of the quadrupole $5s \to \varepsilon d$ transition, where the correlations are negligibly small. The collective character of the behavior of the 5s electrons is maintained only in the vicinity of the threshold of the $4d^{10}$ shell, where the contribution of the quadrupole transition is already small, while the maximum is made possible by the influence of the 4d electrons on the dipole transition. With further increase in q, the relative magnitude of this maximum also declines (see Fig. 9b).

We should note that the dependence of the intershell interaction on q and λ has mainly been studied for those shells of atoms where the dipole polarizability is high. Therefore the major changes occurred specifically in the dipole component of the interaction. Quite possibly, if a transition of a different multipole type λ predominates in the perturbing shell, the intershell interaction will be manifested also at larger values of transferred momenta q. This problem of studying the collective effects in an atom remains open, both on the theoretical and the experimental level.

2.6. Photoionization of sublevels with $j = l \pm 1/2$

Up to now we have neglected the relativistic effects, which affect the partial photoionization cross sections of the individual shells weakly. However, in describing photoprocesses in atoms, one also determines such characteristics as directly involve relativistic corrections to the interaction. One of these is the parameter η, termed the "branching ratio,"[14,19,65] which characterizes the relative probability of ionization of sublevels of a shell having different total angular momenta j.

The existence of electron spin has the result that, in the photoionization of shells with $l \neq 0$, the remaining ion can exist in states differing in total angular momentum, $j = l \pm 1/2$. Within the framework of a one-electron model this can be treated as the removal of an electron from one of the two sublevels of the nl shell having $j_1 = l + 1/2$ or $j_2 = l - 1/2$, which are split by the spin-orbit interaction. The relative probabilities of ionization of these sublevels determine the parameter η: $\eta = \sigma_{l+1/2}/\sigma_{l-1/2}$.

If we neglect relativistic effects including the spin-orbit interaction, the parameter η does not depend on the quantum energy and is determined by the ratio of the populations of these sublevels:

$$\eta_0 = \frac{2j_1+1}{2j_2+1} = \frac{l+1}{l}. \tag{2.19}$$

The difference in the ionization thresholds of the levels with

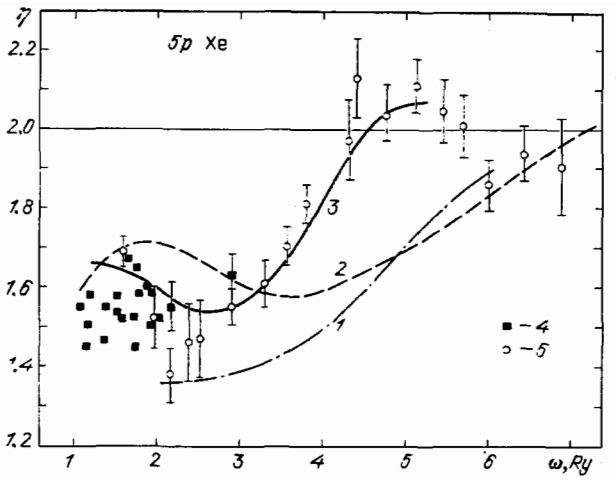

FIG. 10. The parameter $\eta = \sigma_{3/2}/\sigma_{1/2}$ for the 5p electrons of Xe. Calculation: *1*—Dirac-Slater approximation[67]; *2*—Dirac-Fock approximation[70]; *3*—relativistic ARPE method with allowance for the influence of the $4d^{10}$ shell.[55] Experiment: *4*—Ref. 66; *5*—Refs. 67, 68; $\eta_0 = 2$ is the static population ratio.

j_1 and j_2 has enabled measuring the partial photoionization cross sections of these sublevels for np^6 and nd^{10} shells of a number of atoms by methods of photoelectron spectroscopy. In Refs. 65–69 considerable deviations of η from the statistical value η_0 were found. Calculations using the Dirac-Slater[67,68] and Dirac-Fock[70] relativistic wave functions also have led to deviations of η from η_0 and to a dependence of η on ω. However, agreement with experiment has not been attained for many shells, especially np^6, within the framework of single-particle relativistic approximations. It has turned out that, in addition to relativistic effects, multielectron correlations play a large role in governing the populations of the sublevels,[28,55] in particular, the intershell interaction. Concrete calculations within the framework of a relativistic variant of the ARPE[61] have shown its role with the example of the np^6 shells of the noble-gas atoms.

Figure 10 shows the parameter $\eta(\omega)$ for the 5p electrons of Xe. An appreciable deviation of the single-particle calculations from experiment is observed precisely in the vicinity of the ionization threshold of the $4d^{10}$ shell. Only an allowance for the influence of the 4d electrons on the partial cross sections $\sigma_{3/2}$ and $\sigma_{1/2}$ (as we see from Fig. 10, this influence differs) enables obtaining satisfactory agreement with experiment. For the $4p^6$ shell of Kr the influence of the $3d^{10}$ electrons is manifested more weakly[55] than for $5p^6$ of Xe, which agrees with the results presented in Sec. 2.2.

For d electrons it is most essential to take account of the intrashell correlations, since the adjacent shells act on them weakly (apart from the region of autoionization resonances).

Thus the ratio of the partial ionization cross sections of levels of differing j is governed by the joint influence of the relativistic and collective effects.

3. PARTIAL IONIZATION CROSS SECTIONS OF ATOMS WITH UNCLOSED SHELLS

3.1. Specifics of the description of atoms with unclosed shells

The mean radius of atoms with unclosed shells is increased, while the ionization potential is decreased, in comparison with adjacent atoms with filled shells. Consequently the influence of the self-consistent field on the outer electrons is weakened and the role of the direct interaction between the electrons increases. Since here the difference in ionization potentials of the outer and next shells is also decreased, in principle the collective effects in atoms with unclosed shells can be even stronger than in atoms with filled shells.

For atoms with unfilled shells there are considerably fewer theoretical studies at present in which multielectron correlations are taken into account than for atoms with filled shells. The reason for this is a number of difficulties that arise in describing the former.

The theoretical methods used to describe photoprocesses in atoms were first developed and applied mainly only for atoms with filled shells, i.e., electronic systems with an undegenerate ground state. The wave function of such an atom, whose total orbital (L) and spin (S) angular momenta are zero, is represented in the Hartree-Fock approximation in the form of a single determinant composed of single-particle wave functions having the quantum numbers n, l, m, and μ (m and μ are respectively the projections of the orbital and spin angular momenta of the electron). Yet in atoms with an unfilled shell, the wave function of the ground state corresponding to definite values of L and S amounts to a linear combination of determinants differing in the projections m and μ of the single-particle states. In this case the ground state of the atom becomes degenerate in the projections of the angular momenta of the individual electrons entering into the unclosed shell. In particular, this leads to difficulties in applying the ordinary many-body theory. Thus, the single-particle states can no longer be divided into occupied and free states separated by an energy interval. This leads to difficulties in selecting a single-particle basis. Moreover, degeneracy of the ground state leads to appearance of divergent terms in the higher orders of the perturbation-theory series with respect to the interelectronic interaction.

Several methods exist for overcoming these difficulties in many-body theory,[71–73] but most of them are rather complicated for any widespread use in concrete atomic calculations. Computational methods that actually allow one to take account of the multielectron correlations in the process of ionization of atoms with unfilled shells appeared in the middle 60s as a result of generalizing the approximations that are successfully used in atoms with closed shells.[74–80] Theoretically the most systematic ones are the generalizations of the approximation of random phases with exchange[76] and multiparticle perturbation theory,[78] which first showed the great role of the intrashell correlations in the photoionization of the $3p^5$ shell of Cl. The intershell interaction for such atoms has been taken into account as yet in a small number of studies.[16,20,78,80–82]

We note that atoms with half-filled shells can be studied relatively simply by using the very natural apparatus of many-body theory.[81] The physical content of this generalization consists in the following.

According to the Hund rule, atoms in the ground state have the maximum possible spin S. In this case all the electrons in a half-filled shell have identical spin projections μ, e.g., for the sake of definiteness, up (↑). Here all the states with different m are filled and hence the total orbital angular

momentum of the shell and the atom is $L = 0$. The electrons of a half-filled shell can exchange with only half of the electrons from a filled shell. This leads to splitting of the latter into two additional levels that differ in the states having different projections of the electron spins ↑ and ↓. Thus the levels are defined by the quantum numbers n, l, and μ, and remain degenerate only in the projections of the orbital angular momentum m. We can conveniently treat the filled levels as new closed shells, since the Coulomb interaction cannot alter the projection of the spin of an electron and mix the states ↑ and ↓. Therefore it is permissible to apply to such an atom the mathematical apparatus of ordinary many-body theory, in particular, to use the ARPE method.[81] Here one should use as the basis functions the wave functions obtained in the spin-polarized variant of the Hartree-Fock approximation.[83-84]

The spin-orbit interaction mixes the levels with spins ↑ and ↓ (apart from the s electrons). However, as calculations[81,84] show, in atoms with multielectron half-filled shells, the exchange splitting $\Delta_{\uparrow\downarrow}$ for adjacent filled shells is as a rule of an order of magnitude greater than the spin-orbit splitting Δ_{SO} (see Sec. 3.3). Therefore one can neglect them in the first approximation.

The splitting of the atomic shells into the levels ↑ and ↓ leads to additional ionization thresholds, which can be observed in different processes. In particular, one can study the partial cross sections for photoionization of electrons from these levels and study the influence exerted on them by electrons of other levels or shells.

3.2. Atoms with unclosed *ns*- and *np*-shells

The simplest of the atoms with unclosed shells are the alkali metals, which have one outer s electron. Here all the deviation from experiment of the cross sections calculated in the Hartree-Fock approximation should be ascribed to the intershell interaction. In heavy atoms one should also take account of relativistic effects.

The substantial influence of the closed shells in the photoionization of the outer ns electron of alkali atoms has been demonstrated by a set of semiempirical calculations.[27,85-89] In Refs. 27 and 85 the intershell interaction was taken into account by introducing a correction into the dipole matrix element [see (2.12)]. However, such an approximation allows one to describe the photoionization cross section of the ns electron only near its ionization threshold. Other studies[86-89] have employed different model potentials that allow for the influence of the inner shells.

Calculations have also been performed within the framework of methods based on many-body theory. The results of these calculations for the photoionization cross sections of the 4s electrons of K and the 6s electrons of Cs, together with the experimental data[90-92] are presented in Fig. 11. We see from comparing the Hartree-Fock cross sections σ_0^r and σ_0^∇ with the experimental values of σ that the role of the interaction with the inner shells is extremely large. Taking account of the influence of the adjacent $(n-1)p^6$ shell within the framework of the ARPE[16] has fully altered the behavior of the cross sections in K and Cs by increasing it by an order of magnitude as compared with σ_0. However, while satisfactory quantitative agreement was obtained for the K atom (see Fig. 11), for Cs we can speak only of qualitative agreement, since the minimum in the calculated cross section of the 6s electron has been shifted into the prethreshold region.

Calculations within the framework of other approximations have also shown the great role of polarization of the inner electrons.[20,82,93] The ionization cross section of the 6s electrons of the Cs atom has been most carefully studied. Here the influence was taken into account of the autoionization states and relativistic effects. This led to a minimum in the photoionization cross section (see Fig. 11), immediately beyond the I_{6s} threshold and to good agreement with experiment.[90,92]

In the Li atom the intershell interaction is small: the $1s^2$ shell has a small oscillator strength, and hence its influence on the 2s electron is small.[38] In Na the influence of the $2p^6$ shell is quite substantial,[39,93,94] although the matrix elements of the dipole transitions in the continuous $2p \to \varepsilon d$, εs spectrum are not so large as the corresponding quantities in K, Rb, and Cs.

We note that the existence of an outer unclosed ns shell does not substantially affect the intershell interaction between the closed shells in heavy atoms. For example, in the Cs atom the $5s^2$ shell is collectivized in the same way as in Xe by the influence of the $5p^6$ and $4d^{10}$ shells.[16]

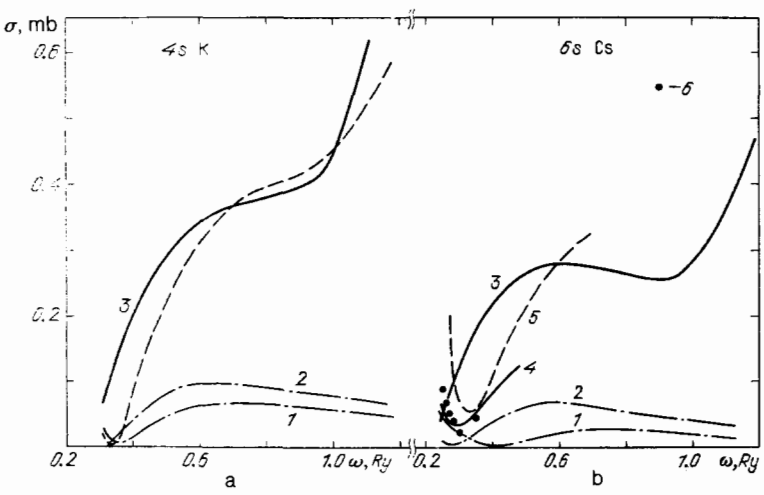

FIG. 11. Photoionization cross section of the 4s electrons of K (a) and the 6s electrons of Cs (b). Theory: *1*, *2*—Hartree-Fock approximation, σ_0^r and σ_0^∇, respectively; *3*—ARPE[16]; *4*—relativistic calculation within the framework of the MPT of the fraction of Cs.[20] Experiment: dotted curves for K and Cs (*5*) from Ref. 90; points *6* from Ref. 92.

The intershell interaction in atoms with unclosed np shells has been studied theoretically and experimentally to a lesser degree than in atoms with filled shells. The reason for this is the computational difficulties mentioned in the previous section and the experimental difficulties involving the preparation of these atoms in the vapor state. There are a number of calculations of the photoionization cross sections of atoms of groups VI and VII of the periodic system in the single-particle approximation[95] and with allowance for correlations.[21,74–80] These calculations indicate that the correlations between electrons—both intrashell and intershell—must be no smaller in these atoms, and sometimes even larger, than in the atoms adjacent in the periodic system having filled shells.

An example is the photoionization cross section of the Cl atom. It is dominated by the contribution of the $3p^5$ electrons, for which, just as in the neighboring atom Ar, the intrashell interaction is large. Taking account of the latter alters the single-particle photoionization cross section in the vicinity of the threshold of the 3p shell by a factor of almost two.[76,78,79] The corresponding change in the cross section for the $3p^6$ shell of Ar is even somewhat smaller. For the next shell—the $3s^2$ shell of Cl, just as in Ar, all the conditions of strong screening by the outer $3p^5$ electrons are practically fulfilled. Figure 12 shows the results of calculating the photoionization cross section of the $3s^2$ shell of Cl within the framework of the MPT. The influence of the $3p^5$ on the $3s^2$ electrons is manifested even more strongly than that of $3p^6$ on the photoionization of $3s^2$ in Ar (see Fig. 4). The existence of the two ionization thresholds ^3P and ^1P manifests the unclosed character of the 3p shell and involves the formation of different final states of the atomic residue.

The study of the correlation interaction in atoms with half-filled np^3 shells is of definite interest. In these atoms, besides the ordinary strong screening by the outer np electrons (as in Cl and Ar) of the deeper ns electrons, a substantial counterinfluence appears. It involves the large role of transitions into the half-filled shell $ns^3np^3 \to ns^1np^4$, which possess a considerable oscillator strength and lie in the region of the discrete spectrum of excitation from the ground state. Taking account of the interaction between this transition and the transition to the continuous spectrum from the

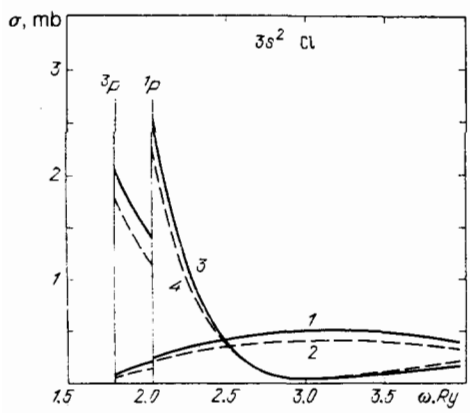

FIG. 12. Photoionization cross section of the $3s^2$ shell of Cl. *1*, *2*—Hartree-Fock approximation, respectively in the r- and ∇-forms; *3*, *4*—the same within the framework of the MPT with allowance for the influence of the $3p^5$ electrons.[78]

np^3 shell leads to very appreciable changes in the ionization cross section of np^3.

For example, in the phosphorus (P) atom, whose structure of the outer shells can be represented in the form ... $3s\uparrow 3s\downarrow 3p^3\uparrow$, the oscillator strength f of the $3s\downarrow \to 3p\downarrow$ dipole transition in the Hartree-Fock approximation is large: $f_{3s\to 3p} = 0.86$. Inclusion of the interaction between the $3s\uparrow$, $3s\downarrow$, and $3p\uparrow$ sublevels leads to substantial changes of all the partial amplitudes and the photoionization cross sections. Thus, the ionization cross section of the $3p^3$ electrons of P with allowance for intrashell correlations rapidly declines from the value $\sigma_{3p} \approx 70$ megabarns at the threshold with increasing energy ω. Under the influence of the discrete transition $3s\downarrow - 3p\downarrow$, the cross section σ_{3p} undergoes qualitative changes: at the threshold it declines by a factor of almost two, then increases with increasing energy and passes through a maximum. The counterinfluence of the $3p^3$ electrons on the phototransitions from the $3s\uparrow$ and $3s\downarrow$ levels causes the oscillator strength of the $3s\downarrow \to 3p\downarrow$ transition to decline by a factor of more than 100 as compared with the Hartree-Fock value and shift into the region of the continuous excitation spectrum of the 3s electrons, leading to a sharp increase in the photoionization cross section σ_{3s} at the threshold and to a shift of the minimum into the higher-energy region.

3.3. Atoms with unclosed *nd*- and *nf*-shells

A powerful maximum beyond the ionization threshold of the unfilled nd shell dominates in the photoabsorption spectrum of the atoms of the transition metals.[96–100] In a number of experimental[96,97] and theoretical[81,101–104] studies, this maximum has been interpreted as a giant autoionization resonance involving a dipole transition of an electron from a deeper filled np^6 shell to free levels in nd and subsequent decay of this state with participation of the electrons of these same levels:

$$np^6nd^N + \gamma \to np^5nd^{N+1} \to np^6nd^{N-1} + e.$$

The great width of the "giant" resonances is $\sim$1–2 eV, which exceeds the ordinary autoionization widths by almost two orders of magnitude, is a consequence of the strong coupling between the adjacent np and nd shells.

The greatest number of studies, both theoretical[81,101–104] and experimental[96–100, 105–108] is devoted to the Mn atom, which has a half-filled $3d^5$ shell. The photoabsorption cross section of the Mn atom in the vicinity of the ionization threshold of the $3p^6$ shell is shown in Fig. 13. The fundamental contribution to the cross section in this region comes from the electrons of the half-filled $3d^5$ shell. However, when one neglects the interaction with transitions from the $3p^6$ shell, the cross section amounts to a monotonic curve (curve *1* in Fig. 13). Taking account of the interaction of these transitions leads to a "giant" resonance and enables one to describe the experiment satisfactorily.

It has been established experimentally that the giant resonance in the cross section has a complicated structure due to the multiplet splitting of the $3p^53d^6$ resonance state. The partial cross sections corresponding to different terms of the final state of the Mn ion have been measured by the method of photoelectron spectroscopy.[98] It turned out that the greatest contribution comes from the transition from the

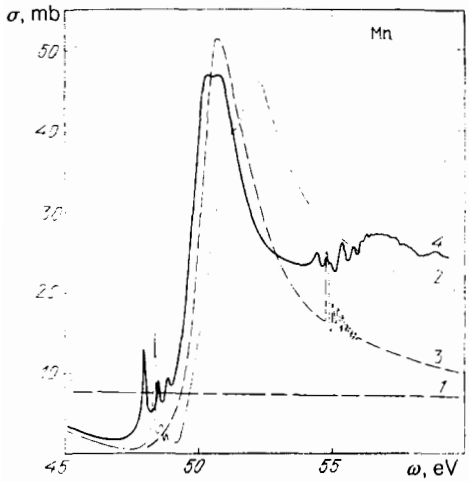

FIG. 13. Photoabsorption cross section of Mn in the vicinity of the threshold of the $3p^6$ shell. *1*—without allowance for the $3p \to 3d$ resonance; *2*, *3*—with allowance for the $3p \to 3d$ transition in different approximations[103,104]; *4*—experiment.[98]

^{6}S Mn I ground state to ^5D Mn II, whose line contour is shown in Fig. 14. The same diagram shows the results of a theoretical calculation within the framework of the spin-polarized variant of the ARPE.[81] The structure of the outer shells of the ground state of Mn can be written as[81]:

$$\ldots 3s^1\uparrow 3s^1\downarrow 3p^3\uparrow 3p^3\downarrow 3d^5\uparrow 4s^1\uparrow 4s^1\downarrow\ (^6S).$$

Then the transition that makes the main contribution to the giant resonance is represented as follows:

$$3p^3\uparrow 3p^3\downarrow 3d^5\uparrow\ (^6S)+\gamma\to 3p^3\uparrow 3p^2\downarrow 3d^5\uparrow 3d^1\downarrow\ (^6P)\to$$
$$\to 3p^3\uparrow 3p^3\downarrow 3d^4\uparrow\ (^5D)\,\varepsilon f\uparrow\ (^6P).$$

The width of this resonance is somewhat smaller (experiment[98] yields $\Gamma_e \approx 1.3$ eV, while calculation in the ARPE[81] yields $\Gamma = 1.4$ eV) than in the photoabsorption spectrum ($\Gamma \sim 2$ eV). Yet it remains very large in comparison with the value typical for ordinary autoionization lines.

Figure 14b shows the contribution of the same resonance transition to the photoionization cross section of the Cr atom, which has two half-filled shells in the ground state: $\ldots 3p^3\uparrow 3p^3\downarrow 3d^5\uparrow 4s^1\uparrow\ (^7S)$.

Also the maximum in the partial photoionization cross sections of the outer 4s electrons has been studied experimentally[98] and theoretically[104] within the framework of the MPT. Their contribution to the total cross section is 20 times smaller than the ionization cross section of the 3d electrons.

We note that the splitting of the levels of the one shell with spins up ↑ and down ↓ caused by the exchange interaction with the $3d^5\uparrow$ shell is rather large. In Mn it amounts to $\Delta_{\uparrow\downarrow} = 1$ eV for the 4s shell and $\Delta_{\uparrow\downarrow} = 13$ eV for the 3p shell. Here the value of $\Delta_{\uparrow\downarrow}$ for the 3p electrons is considerably greater than the splitting caused by the spin-orbit interaction $\Delta_{SO} = 1.4$ eV. Thus one can experimentally distinguish the partial contributions of these levels to the photoionization cross section of a given shell.[109,110]

In the other atoms of the fourth period, photoionization generally occurs in an analogous way with active participation of the unclosed 3d shell, only the cross sections have a far more complicated resonance structure than in Mn.[99,100] The latter substantially complicates the theoretical study of the photoionization of these atoms.

In going to heavier atoms with 4d or 5d shells being filled, the width of the giant autoionization maximum is increased. Thus, in the Tc atom with a half-filled $4d^5$ shell, the calculated width of the resonance exceeds 2 eV.[81]

An even greater interaction between filled and unfilled shells is observed in atoms with a 4f shell being filled, where the resonance arises from a discrete transition of the 4d electron: $4d^{10}4f^N \to 4d^9 4f^{N+1}$. The total and partial photoionization cross sections of the atoms of the rare-earth elements (see Ref. 47 and the references cited there) have exhibited broad ($\Gamma \sim 10$–20 eV) resonances having a very complex structure. The measurements were mainly performed on metals, but there is no doubt that the photoionization cross sections of the isolated atoms are close in magnitude and shape, since the 4d and 4f electrons in the metal are not collectivized. We note that the behavior of the cross section, which in shape recalls a giant resonance, is observed even in La (outer shells $6s^2 5d^1$).[111] However, there the phenomenon arises from the transition $4d \to \varepsilon f$ to the continuous f-electron spectrum,[112] and correspondingly its effect on the outer shells is analogous to the influence of $4d^{10}$ in Xe, Cs, and Ba (see Sec. 2.2). In going to the following elements, the discrete transition to free levels in the 4f shell now acquires

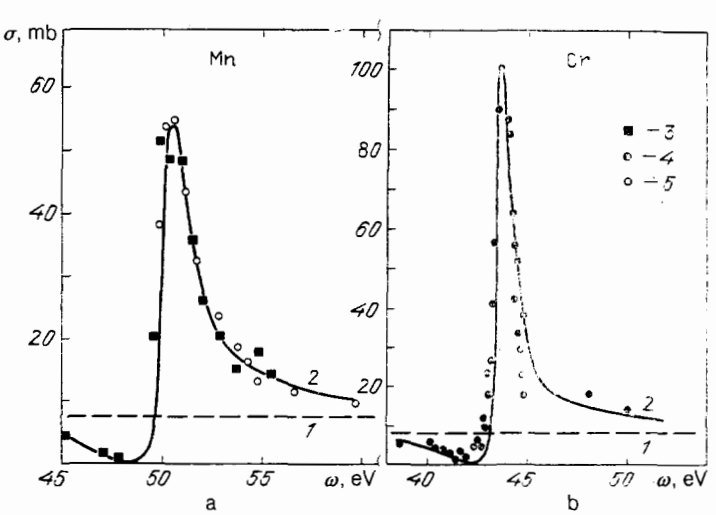

FIG. 14. Photoionization cross section of the $3d^5$ shells of Mn and Cr in the vicinity of the resonance $3p\downarrow \to 3d\downarrow$ transition. Theory: *1*, *2*—ARPE without and with allowance for resonance, respectively.[81] Experiment: *3*—Ref. 98; *4*—Ref. 107 normalized to the calculated maximum.

the major oscillator strength and governs the photoabsorption spectrum and the intershell interaction over a broad energy range.

4. ANGULAR DISTRIBUTION AND POLARIZATION OF PHOTOELECTRONS

4.1. Angular distribution of photoelectrons

The photoionization cross section is determined by the squares of the moduli of the dipole amplitudes. Hence it does not depend on the signs of their real and imaginary components. The parameters that describe the angular distribution and polarization of the photoelectrons are determined by the transition amplitudes themselves, together with the phases of the scattering of the photoelectron in the field of the ion. Therefore the study of the angular distribution and polarization of photoelectrons in principle yields more detailed information on dipole transitions in atoms than the study of the partial cross-sections does.

Let us study the angular distribution of photoelectrons ejected from a shell having the quantum numbers n and l. Upon illuminating an unpolarized atom with unpolarized light, it is determined by the expression[113]

$$\frac{d\sigma_{nl}}{d\Omega}=\frac{\sigma_{nl}(\omega)}{4\pi}\left[1-\frac{1}{2}\beta_{nl}(\omega)\,P_2(\cos\theta)\right]. \qquad (4.1)$$

Here $P_2(\cos\theta)$ is the Legendre polynomial, $d\Omega$ is the element of solid angle of emergence of the photoelectron, and σ_{nl} is the total photoionization cross-section of the nl shell:

$$\sigma_{nl}(\omega)=\sigma_{nl,\varepsilon l+1}(\omega)+\sigma_{nl,\varepsilon l-1}(\omega). \qquad (4.2)$$

Here $\sigma_{nl,\varepsilon l\pm 1}$ is determined by Eqs. (2.1). The angular-anisotropy parameter $\beta_{nl}(\omega)$ is expressed in terms of the dipole matrix elements $D_{l\pm 1}=\langle\varepsilon l\pm 1|\hat{D}|nl\rangle$, which are determined by Eqs. (2.2)–(2.7) and the phases of scattering of the photoelectrons with the angular momenta $l\pm 1$ $-\delta_{l\pm 1}$ [16,113]:

$$\beta_{nl}(\omega)=\frac{1}{(2l+1)(|D_{l-1}|^2+|D_{l+1}|^2)}\times\Big[(l-1)\,|D_{l-1}|^2+(l+2)\,|D_{l+1}|^2+6\,[l(l+1)]^{1/2}\,\mathrm{Re}\Big\{D_{l+1}D^*_{l-1}\exp\Big[i(\delta_{l+1}-\delta_{l-1})\Big]\Big\}\Big]. \qquad (4.3)$$

The energy-dependence of β in the angular distribution appears as a result of interference of the contributions of the two transitions $nl\to\varepsilon l+1$ and $nl\to\varepsilon l-1$. The amplitudes $D_{l\pm 1}$ of these transitions and their dependence on the energy ω, as was shown above, can change substantially upon taking account of the intra- and intershell correlations. However, as a rule, the intrashell interaction does not lead to qualitative changes in the dependence of the anisotropy parameter β on ω as compared with the single-particle calculation.[16] The situation differs when we take account of the intershell interaction: the amplitude of the transition can acquire additional zeros, maxima, and minima, which is reflected in the quantitative and qualitative changes in the behavior of β as a function of ω.

As an example, let us examine the angular distribution of electrons from the $5p^6$ shell of Xe, which has been studied in considerable detail, both theoretically[41,114] and experimentally.[115–119] The amplitude of the main dipole transition $5p\to\varepsilon d$ under the influence of the $4d^{10}$ shell depends very essentially on the energy (see Fig. 2). The influence of the $4d^{10}$ electrons on the amplitude of $5p\to\varepsilon s$ is far smaller. However, even it is manifested appreciably in $\beta_{5p}(\omega)$.[114] The phase difference $(\delta_{l+1}-\delta_{l-1})$ is determined in the course of the calculation of the corresponding Hartree-Fock wave functions and is a smooth function of the energy.[114]

For Xe the dependence of β_{5p} on the energy of the quantum is shown in Fig. 15. We see that the experimental data agree well with the results of the theoretical calculations that take account of the influence of the $4d^{10}$ shell, which has led to an additional oscillation in β.

The behavior of the amplitudes and phases of the wave functions for the $5p^6$ shells of the atoms Cs and Ba resembles that which takes place in Xe and leads to the same additional oscillation in the anisotropy parameter as in the case of Xe.[114]

The strong influence of the $4d^{10}$ shell extends not only to the shells exterior to it, but also to the deeper ones, in particular, the $4p^6$ shell. Calculations within the framework of the ARPE for the $4p^6$ shell of Pd and Xe have also shown considerable changes in the $\beta_{4p}(\omega)$ relationship upon taking account of the 4d electrons[2)].[114] As compared with the $4d^{10}$ shell, $3d^{10}$ exerts a smaller influence on the neighboring $4p^6$ and $3p^6$ shells.[120]

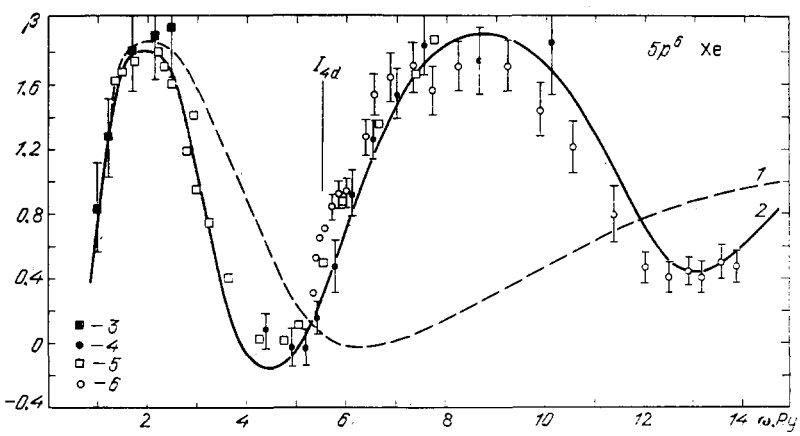

FIG. 15. The anisotropy parameter β_{5p} of the $5p^6$ shell of Xe. Theory: *1*—without allowance for the intershell interaction; *2*—with allowance for the influence of the $4d^{10}$ shell.[114] Experiment: *3*—Ref. 115; *4*—Ref. 117; *5*—Ref. 118; *6*—Ref. 119.

4.2. Angular distribution of photoelectrons from *ns*-shells

In studying the angular distribution of photoelectrons from *ns* shells we face the joint manifestation of collective and relativistic effects in the atom.[19,121,122]

In the nonrelativistic approximation the electrons of s shells possess only one dipole transition $ns \to \varepsilon p$. Therefore we find from Eq. (4.3) that $\beta_{ns} = 2$ at all quantum energies ω.

However, the total angular momentum of the leaving photoelectron can acquire the values $j_1 = 3/2$ and $j_2 = 1/2$. The wave functions corresponding to these states have different radial and energy dependences and scattering phases, owing to the spin-orbit interaction. The waves with $j_1 = 3/2$ and $j_2 = 1/2$ interfere with one another, which leads to a dependence of the angular distribution on the photon energy. When we take account of relativistic effects, the angular anisotropy parameter β for the s electrons has the form[123]

$$\beta_{ns}(\omega) = \frac{|D_{3/2}|^2 + 2\sqrt{2}\,\mathrm{Re}\,\{D_{1/2}D^*_{3/2}\exp[i(\delta_{1/2}-\delta_{3/2})]\}}{|D_{1/2}|^2 + |D_{3/2}|^2}. \quad (4.4)$$

Here $D_{3/2(1/2)} = \langle \varepsilon p_{3/2(1/2)} | \hat{D} | ns \rangle$ are the matrix elements of the transition to the state with $j = 3/2(1/2)$, while $\delta_{3/2(1/2)}$ are the corresponding phases of elastic scattering of the photoelectron in the field of the ion.

Calculations of the parameter $\beta_{ns}(\omega)$ in the single-particle Dirac-Fock calculation have been performed for the s shells of a number of atoms (Ref. 121 and the references cited there). Calculations taking account of multielectron correlations, including the intershell interaction have been performed within the framework of various methods for the outer *ns* shells of the atoms of the alkali[20] and alkaline-earth[28] metals and the noble gases.[25,55,61,124] The angular distributions of the 4s electrons in Kr[125,126] and the 5s electrons in Xe[60,127–129] have been studied experimentally in the greatest detail.

Owing to the spin-orbit interaction, the amplitudes (or their real components) of $D_{3/2}$ and $D_{1/2}$ vanish at different energies, which leads to a strong variation in the behavior of $\beta_{ns}(\omega)$. Figure 16 shows the experimental data and the results of theoretical calculations of the parameter β_{5s} for the Xe atom. We note that in the single-particle Dirac-Fock approximation the characteristic minimum in β is seemingly shifted into the prethreshold region, which corresponds to the behavior of the single-particle photoionization cross section σ_{5s} (see Fig. 6). When one allows for the influence of the $5p^6$ shell (the phases $\delta_{1/2}$ and $\delta_{3/2}$ remain as before), the minimum in the cross section, and correspondingly in β_{5s}, shifts by an energy ~ 2 Ry beyond the threshold of the $5s^2$ shell (curve *2* in Fig. 16). A position of the minimum in β_{5s} corresponding to the experimental position is attained only when one takes account simultaneously of the influence of the $5p^6$ and $4d^{10}$ shells. The best agreement with experiment is obtained within the framework of the relativistic variant of the time-dependent local-density approximation (TDLDA).[25]

An analogous pattern is observed for $\beta_{4s}(\omega)$ in Kr. An essential point is that here the latest experimental data[126] show a difference of the results of calculations within the framework of the relativistic ARPE and TDLDA.

A strong influence of the intershell interaction is also manifested in the angular distribution of the valence s electrons of the atoms of the alkali and alkaline-earth metals. There are no experimental measurements of β_{ns} for the alkali atoms at present. However, a substantial role of the inner p^6 shells can be seen from comparing the relativistic calculations within the framework of single-particle approximations[121] and with account taken of the correlations. Let us say that, for the Cs atom, allowing for the influence of the $5p^6$ shell shifts the deep minimum in the parameter β that reaches practically to a value of -1 by an amount greater than 1 eV toward the ionization threshold of the 6s shell. This shift lies in a direction opposite to the shift of the minimum of β_{5s} of Xe, which agrees with the qualitative picture of the influence of an inner shell (see Sec. 2.4).

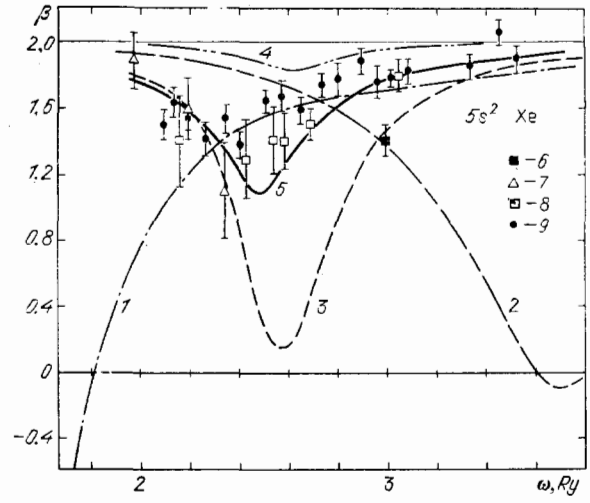

FIG. 16. The anisotropy parameter $\beta_{5s}(\omega)$ for the $5s^2$ electrons of Xe. Theory: *1*—Dirac-Fock approximation[121]; *2, 3*—relativistic variant of the ARPE with allowance for the interaction of two ($5p^6 + 5s^2$) and three ($5p^6 + 5s^2 + 4d^{10}$) shells, respectively[55]; *4*—*R*-matrix method[61]; *5*—relativistic variant of the TDLDA.[25] Experiment: *6*—Ref. 127; *7*—Ref. 128; *8*—Ref. 129; *9*—Ref. 60.

For the atoms of the alkaline-earth metals, on the whole also only theoretical calculations of $\beta_{ns}(\omega)$ exist.[28,130] An exception is the atom of Hg, for which a set of experimental points has been obtained for $\beta_{6s}(\omega)$.[131,132] However, one cannot speak of good agreement between experiment and theory.

4.3. Features of the angular distribution of photoelectrons in atoms with half-filled shells

The interaction with transitions from deeper shells to free levels in an unfilled shell exerts an especially great influence on the dependence of the anisotropy parameter of the photoelectrons from unclosed shells on ω. It was noted above (see Sec. 3.3) that these transitions lead to giant resonances of great width in the photoabsorption cross sections of atoms with nd^N and nf^N shells. They are also manifested in the angular distribution, which leads to a resonance-type dependence of the angular anisotropy parameter $\beta(\omega)$ on ω.

Let us examine these and certain other features of angular distributions in atoms with unclosed shells involving the intershell interaction with the example of the Mn atom. A set of experimental[107–110] and theoretical[81,104,133] studies exist for it on determining the energy dependence $\beta(\omega)$ for photoelectrons from different shells.

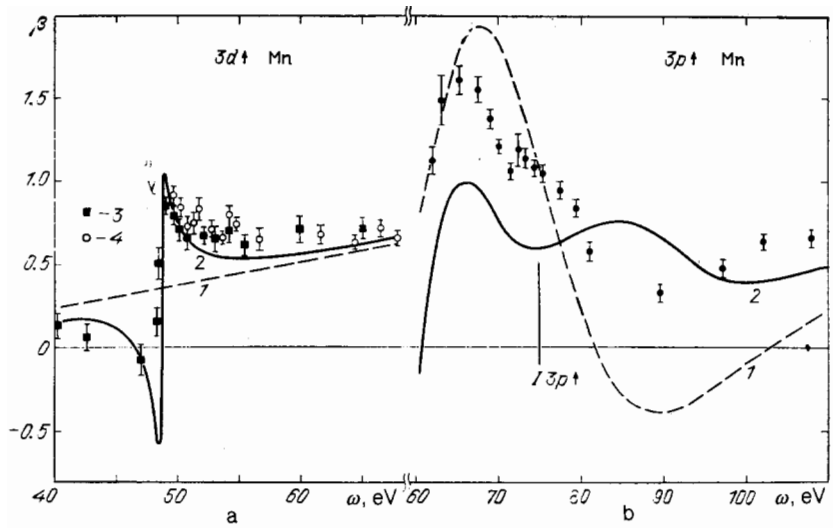

FIG. 17. Anisotropy parameters β for the $3d^5\uparrow$ (a) and $3p^3\downarrow$ (b) electrons in Mn. a) *1*, *2*—calculation without and with allowance for the influence of the resonance transition $3p\downarrow \to 3d\downarrow$,[81] respectively; experiment: *3*—Ref. 108; *4*—Ref. 107. b) *1*—spin-polarized Hartree-Fock approximation; *2*—with allowance for the influence of the $3d^5\uparrow$ electrons; —with allowance for the influence of the $3d\uparrow$ and $3p\uparrow$ electrons[133]; experiment—Refs. 109, 110.

In the ground state of Mn all the electrons in the half-filled $3d^5$ shell have identical spin projections $\mu(\uparrow)$, while all the states with differing m are filled. In this case the parameter β for the $3d^5$ photoelectrons is determined by the ordinary formula (4.3). The calculations that have been performed within the framework of the ARPE[81] and MPT[104] have clearly shown the manifestation of the giant autoionization resonance $3p^63d^5 \to 3p^53d^6$ (see Sec. 3.3) also in the angular distribution. Figure 17a shows the results of the calculations of the $\beta(\omega)$ relationship and the experimental data,[107,108] which agree well with one another.

The theoretical study of the partial photoionization cross sections and the parameter $\beta(\omega)$ for each of the $3p^3\uparrow$ and $3p^3\downarrow$ levels in Cr and Mn[133] revealed a strong interaction between the $3p\uparrow$ and $3p\downarrow$ electrons themselves, in addition to the influence exerted by the $3d^5\uparrow$ shell. At the threshold of the $3p^3\uparrow$ level deeper in energy owing to excitation of its electrons, nonmonotonicity arises in the amplitude of the $3p\downarrow \to \varepsilon d\downarrow$ transition and leads to an extra maximum in the parameter $\beta_{3p\downarrow}$ (Fig. 17b). Recent experimental measurements[109] of the angular distribution of the 3p photoelectrons have revealed an extra maximum, which serves as a definite confirmation of the great role of the interaction between the two levels. Only qualitative agreement of theory with experiment exists. Perhaps the quantitative deviation of the calculated results from the experimental data involves the fact that the $3p\uparrow$ level (term of the ionic state ^5P) has a complex non-single-electron nature.[110] In the photoelectron spectrum[110] it is manifested only as a very weak structure and has a greater width than the $3p\downarrow$ level, which is represented in the spectrum by a distinct maximum. The exact mechanism of the interlevel interaction of the electrons is still not fully clear in this case.

4.4. Polarization of photoelectrons

Studying the polarization of photoelectrons makes it possible to obtain even more detailed information on the features of behavior of the dipole amplitude. The experimental determination of the partial cross sections, of the angular distribution of the photoelectrons, and of their polarization forms the so-called complete quantum-mechanical experiment, which enables measuring all the amplitudes characterizing the photoionization, with their real and imaginary components.

The degree of polarization P of the electrons is defined by the preferential directionality of their spins:

$$P = \frac{N_\uparrow - N_\downarrow}{N_\uparrow + N_\downarrow}. \tag{4.5}$$

Here $N_\uparrow$ and $N_\downarrow$ are the numbers of photoelectrons having a spin direction along and against the chosen axis. Evidently the polarization differs from zero only when one takes account of the spin-orbit interaction. However, its magnitude and behavior as a function of the energy depend on the correlation interaction in the atoms, since the numbers of photoelectrons $N_\uparrow$ and $N_\downarrow$ are determined by the dipole amplitudes. A number of authors[134–137] have derived expressions for P for the cases of an arbitrary atom and incident polarized and unpolarized photons. It was shown that the photoelectrons emerging at any angle generally possess a non-zero degree of polarization, even with incident unpolarized light.

In the general case the energy-dependence of the degree of polarization is given by a rather complicated expression,[136] which is simplified for atoms with filled shells. In the photoionization of an atom with filled shells by unpolarized light, the degree of polarization of the ejected electrons can be written as follows[136]:

$$P_j = -\frac{\eta_j (\mathbf{S}[\boldsymbol{\varkappa}\mathbf{k}])(\boldsymbol{\varkappa}\mathbf{k})}{1-(1/2)\beta[(3/2)(\boldsymbol{\varkappa}\mathbf{k})^2-(1/2)]}. \tag{4.6}$$

Here $\mathbf{S}$, $\boldsymbol{\varkappa}$, and $\mathbf{k}$ are unit vectors lying parallel to the spin of the electron, the momentum of the photon, and the momentum of the electron, respectively. The parameter β is determined by (3.3), and the parameter η_j, just like β, is expressed in terms of the dipole matrix elements $D_{l\pm1}$ and the phases $\delta_{l\pm1}$ of elastic scattering[136]:

$$\eta_j = \frac{(-1)^{j-l-1/2}}{2j+1} \cdot \frac{3[l(l+1)]^{1/2}\,\mathrm{Im}\{D_{l+1}D^*_{l-1}\exp[i(\delta_{l+1}-\delta_{l-1})]\}}{|D_{l+1}|^2+|D_{l-1}|^2}. \tag{4.7}$$

In deriving (4.6) and (4.7) it was assumed for simplicity that the matrix elements and phases can be calculated in the LS-coupling, while the spin-orbit interaction leads only to splitting of the nl shell into two subshells with total angular momenta $j = l + 1/2$ and $j = l - 1/2$.

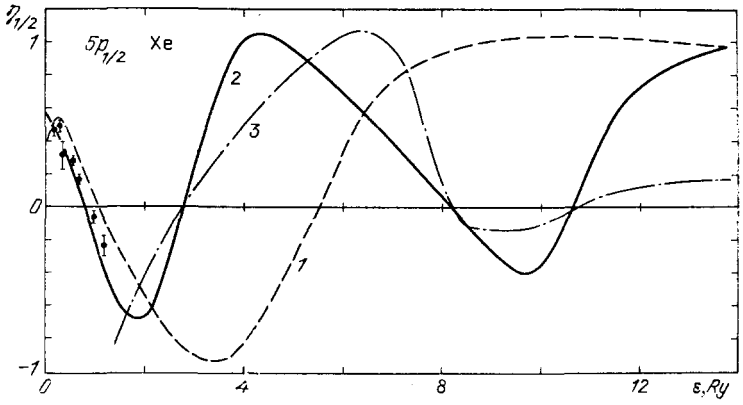

FIG. 18. Dependence of the parameter $\eta_{1/2}$ on the energy of the photoelectron for the $5p_{1/2}$ subshell of Xe. Theory: *1, 2*—ARPE, respectively without and with allowance for the influence of the $4d^{10}$ shell[136]; *3*—amplitude of the $5p \to \varepsilon d$ transition in relative units; experiment—Refs. 138, 139.

As we see from (4.6), the degree of polarization depends on the angle of emergence of the photoelectron. It generally differs from zero and is proportional to the parameter η_j. Since the latter is expressed directly in terms of the product of amplitudes, the degree of polarization of the photoelectrons as a function of the energy is highly sensitive to variations of the amplitudes of the dipole transitions, and hence also to manifestations of the intershell interaction.

Figure 18 shows the parameter $\eta_{1/2}$ for the $5p_{1/2}$ subshell of Xe as a function of the energy. The amplitude of the $5p \to \varepsilon d$ transition undergoes strong variations under the influence of the $4d^{10}$ shell (see Fig. 2), which have been expressed in the $P_{1/2}(\omega)$ relationship. The degree of polarization literally copies all the features of the $5p \to \varepsilon d$ amplitude. The amplitude of the $5p \to \varepsilon s$ transition varies monotonically with increasing ε, and the influence of the 4d electrons does not change its sign. An exception is the first zero of P, which arises from the passage of the phase difference through π. The existing experimental data[138,139] agree well with the calculated values. Unfortunately no measurements have yet been performed in the energy region where the extra zeros in $\eta_{1/2}$ appeared. We note that a relativistic calculation within the framework of the ARPE[122] proved very close to the nonrelativistic results.

4.5. Angular anisotropy of Auger electrons

In the process of photoionization of inner atomic shells with a total angular momentum $j > 1/2\,(l > 0)$, the ions being produced have a definite alignment (preferential orientation of the total angular momentum j) along the direction of the incident photon beam.[140] This alignment, which arises from the nonuniform population of the states having differing projections of the total angular momentum **M** of the ion, is manifested in an anisotropy of the angular distribution of the emitted photons or Auger electrons emitted upon decay of the vacancy. The alignment of the ions depends on the squares of the dipole amplitudes[141] in a way differing from the photoionization cross section. Hence the measurement of the angular anisotropy of the electrons or photons also yields supplementary, independent information on the photoionization process.

The angular distribution of the Auger electrons is determined by the relationship[140]

$$W \sim 1 + A_2^j(\omega)\, P_2(\cos\theta). \tag{4.8}$$

Here θ is the angle between the momenta of the incident photon and the Auger electron, $j = l \pm 1/2$, while the parameter A_2^j characterizes the degree of alignment and is written in terms of the dipole matrix elements[141]:

$$A_2^j(\omega) = (-1)^{j+l+1/2}(2l+1)\left[\frac{3}{2}(2j+1)\right]^{1/2}\begin{Bmatrix} l & 2 & l \\ j & \frac{1}{2} & j \end{Bmatrix} \times \frac{\begin{Bmatrix} l & 2 & l \\ 1 & l-1 & 1 \end{Bmatrix} |D_{l-1}|^2 + \begin{Bmatrix} l & 2 & l \\ 1 & l+1 & 1 \end{Bmatrix} |D_{l+1}|^2}{|D_{l-1}|^2 + |D_{l+1}|^2}. \tag{4.9}$$

Thus the variation of the magnitudes of the dipole amplitudes, including that under the influence of the intershell interaction, can be substantially reflected in the angular distribution of the Auger electrons.

Naturally, the alignment of the ions is manifested also in the photoionization of the outer shells with $j > 1/2$, in particular the $5p_{3/2}$ subshell of Xe, which is strongly influenced by the $4d^{10}$ shell (see Fig. 2). However, experimental study of the degree of alignment is highly impeded by the lack of decay products.

The situation differs in the Ba atom, where a vacancy in the $5p_{3/2}$ subshell, which is also highly sensitive to the influence of the $4d^{10}$ electrons, has the possibility of decaying with ejection of Auger electrons from the $6s^2$ shell, whose anisotropy can be determined experimentally. Figure 19 shows the results of calculating the parameter $A_2^{3/2}$ for the $5p_{3/2}$ subshell of Ba, from which we see that the intrashell interaction, although it is large and strongly alters the par-

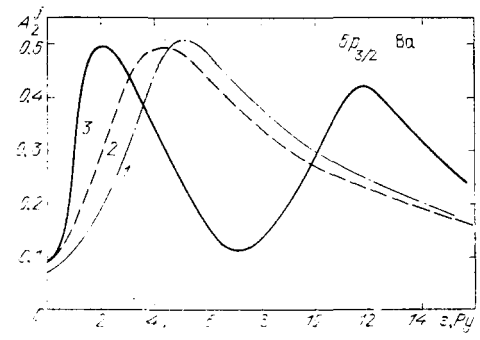

FIG. 19. Angular anisotropy parameter $A_2^{3/2}$ of emergence of the Auger electrons emitted upon photoionization of the $5p_{3/2}$ subshell of Ba. Calculated curves: *1*—Hartree-Fock approximation; *2*—ARPE with allowance for intrashell correlations; *3*—ARPE with allowance for the influence of the $4d^{10}$ shell.[142]

tial photoionization cross section, does not lead to appreciable changes in A_2^j. Taking account of the influence of the deeper $4d^{10}$ shell led to an additional oscillation in $A_2^{3/2}$,[142] similar to that manifested in the parameter β for Xe, Cs, and Ba itself.[114]

5. READJUSTMENT OF ELECTRON SHELLS

The collective effects in the photoionization of inner shells near their threshold are more complicated in character than for the outer shells. In addition to the forced mutual ordered motion of the electrons of one or several adjacent shells that occurs under the influence of an external electromagnetic field, various relaxation processes occur.

Relaxation, or readjustment, is a complex, dynamic process reflecting the reaction of the atomic electrons to the appearance of a vacancy in one of the shells and its subsequent decay. Taking account of readjustment leads to changes in the photoionization amplitudes and in the interaction among the electrons. In Sec. 5 we shall treat the fundamental features of the influence of readjustment on the intershell interaction in the photoionization of atoms.

5.1. "Static" readjustment of outer electron shells

It is evident from qualitative considerations that the influence of readjustment of an atom to ionization is greatest near the threshold of an inner shell. In fact, in the time during which a slow photoelectron leaves the atom, the remaining electrons succeed in "sensing" and "adjusting" to the change in the field caused by the production of a vacancy and its subsequent decay. Thus a slow photoelectron moves in a time-varying field formed by the nucleus and the readjusting electrons of the atom.

Taking account of readjustment fully amounts to a highly difficult problem. However, a number of cases exist in which one can restrict the treatment to relatively simple approximations.

Readjustment is manifested not only in the change in the wave function of the departing electron, but also in the deviation of the ionization energy from the Hartree-Fock value of the energy of the level. Hence, let us estimate the time in which the electron shells of the atom are readjusted owing to creation of a vacancy, starting from the difference of the true ionization potential I_{nl} from the corresponding energy value E_{nl} of the electron in the Hartree-Fock approximation for the nl shell:

$$\tau_{nl} \sim |E_{nl}+I_{nl}|^{-1}. \tag{5.1}$$

If $|E_{nl}|=I_{nl}$, readjustment does not occur ($\tau_{nl}\to\infty$). The time for readjustment of the atomic shells involving the decay of a vacancy in an inner shell can be determined from the relationship $T_{nl}\sim 1/\Gamma_{nl}$, where Γ_{nl} is the total width of the vacancy in the nl shell. For a photoelectron having a velocity $v=(2\varepsilon)^{1/2}$ ($\varepsilon>0$ is its energy), the time for leaving the atom is $t\sim R/(2\varepsilon)^{1/2}$, where R is the radius of the atom. Evidently readjustment is important when $t\gg T_{nl}, \tau_{nl}$.

The study of the influence of readjustment is considerably simplified in the case in which the condition is satisfied that

$$T_{nl}\gg t\gg \tau_{nl}. \tag{5.2}$$

Here one can neglect the influence of the decay of the vacancy on the photoionization process, while the motion of the photoelectron from the instant of its creation can be treated in the static self-consistent field of an already completely readjusted atomic residue with a hole in the nl shell. This constitutes the content of the "static"-readjustment approximation.[45] It is taken into account with an appropriate choice of the single-particle wave functions of the electron and the hole, which subsequently can be used in the ARPE equations or in other methods.

The use of the ARPE method thus generalized leads to taking account of diagrams that lie outside the framework of the ARPE [see (2.4) and (2.6)]. In the lowest order of perturbation theory, these diagrams have the form

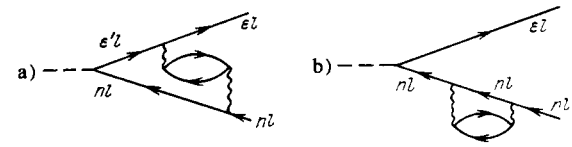

(5.3)

Here the amplitude a) takes account of the screening by the remaining electrons of the interaction between the photoelectron and the hole ($\varepsilon' l'$; $\varepsilon l'$), and the amplitude b) takes account of the correction to the energy and the wave function of the hole state ($\varepsilon l'$). The screening diminishes the photoionization amplitude, and correspondingly diminishes the cross-section near the threshold. Concrete calculations for a number of intermediate and inner shells[45] have shown the substantiality of the influence of static readjustment on the photoionization cross-section. It has been shown with the examples of the $4d^{10}$ shells of Xe, Cs, and Ba[45] and La[112] that the influence of readjustment becomes more substantial as the photoionization cross section becomes concentrated to a greater degree near the ionization threshold. The more the maximum in the cross section is shifted away from the threshold, the smaller is the role of readjustment.

The decrease in the photoionization amplitudes of the inner shells arising from readjustment leads to a decrease in their influence on the photoionization of the outer shells. The necessary condition for readjustment to influence the intershell interaction proves to be the following time relationship:

$$\tau_{nl} \lesssim t_{nl}. \tag{5.4}$$

Here t_{nl} is the "lifetime" of the intermediate state of the interacting shells, which can be estimated by using the relationship

$$t_{nl} \sim \frac{1}{\omega-\varepsilon'-I_{nl}}. \tag{5.5}$$

Here ε' is the energy of the electron in the intermediate state. Since the readjustment is significant for small ε', evidently the influence of readjustment of the inner shell nl is manifested in the ionization cross-section of an outer shell only in the vicinity of its ionization threshold $\omega\sim I_{nl}$.

Figure 20 shows the photoionization cross-section of the $5p^6$ shell of Ba with allowance for the "unreadjusted" and "readjusted" $4d^{10}$ shell as calculated within the framework of the ARPE.[45] Analogous results for Ba have also been obtained in the TDLDA method.[23] We see that taking account of readjustment can alter severalfold the strength of the intershell interaction.

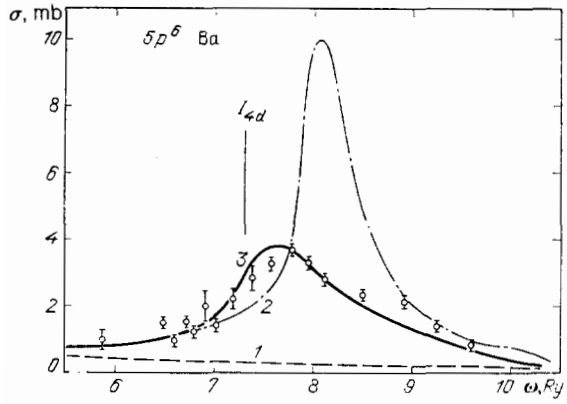

FIG. 20. Photoionization cross section of the $5p^6$ shell of Ba in the vicinity of the $4d^{10}$ threshold. Theory: *1*—without allowance for the influence of the $4d^{10}$ shell; *2*—ARPE with allowance for the influence of the $4d^{10}$ shell; *3*—with allowance for the readjusted $4d^{10}$ shell[45]; the experimental values[44] are normalized to the maximum of the cross section.

5.2. Decay of vacancies and post-collision interaction

The static-readjustment approximation becomes inapplicable when the lifetime of a vacancy T_{nl} is comparable with the emergence time t of the photoelectron from the atom. In this case a low-energy photoelectron cannot travel far enough from the remaining ion in the decay time of the hole, and it "senses" the changed field of the ion arising from decay. In Auger decay this new field corresponds to a charge greater by unity than the initial field formed upon absorbing a quantum. Owing to the enhanced attraction, the slow electron in the new field has an energy smaller than that which it would have if we neglect the decay of the vacancy. The fast Auger electron bears away the released energy.

This phenomenon, which involves the redistribution of energy between the photoelectron and the Auger electron, amounts to a strong correlation effect, and has been termed the post-collision interaction (PCI) (see Ref. 57 and the references cited there). This effect substantially alters the amplitude, and correspondingly the cross section, of photoionization, as well as the energy distribution of the Auger electrons and the photoelectrons. Recently the effects of the post-collision interaction have been intensively studied, both experimentally,[143–145] and theoretically.[146–151]

The analysis of this correlation effect is simplified when the width Γ_j of a deep vacancy is not too large, and a rather fast electron is produced by its decay, so that we can neglect the interaction with the slow photoelectron. We can write the corresponding photoionization amplitude with allowance for the post-collision interaction in the form

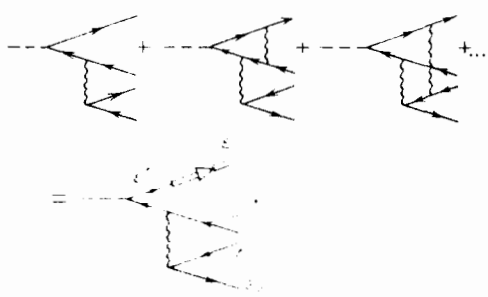

(5.6)

Here the double line denotes the wave function of the photoelectron $|\tilde{\varepsilon}\rangle$ having the energy $\tilde{\varepsilon}$ calculated in the field of the doubly charged ion having the holes p and k. We shall represent the analytic expression in the form[149]

$$D_{\tilde{\varepsilon}\varepsilon_f} = \left(\sum, \int\right)_{\varepsilon' \geqslant F} \langle j \mid \hat{D} \mid \varepsilon' \rangle \frac{\langle j\varepsilon_f \mid \hat{U} \mid kp \rangle \langle \varepsilon' \mid \tilde{\varepsilon} \rangle}{\omega - \varepsilon' - E_j + i(\Gamma_j/2)}. \quad (5.7)$$

Here the first factor in the integrand is determined from (2.2) or (2.6), $\langle j\varepsilon_f | \hat{U} | kp \rangle$ is the matrix element for Auger decay of vacancy j determined analogously to (2.3), and the last factor, $\langle \varepsilon' | \tilde{\varepsilon} \rangle$ is the overlap integral of the wave functions of the electron $\langle \varepsilon' |$ (in the field with the hole j) and $|\tilde{\varepsilon}\rangle$.

When one takes account of the post-collision interaction, the energy distribution of the Auger electrons is broadened and becomes asymmetric instead of having the ordinary symmetric Breit-Wigner contour. The appearance of an asymmetric contour means that the photoionization process at low energies above the threshold of the inner shell cannot be represented as occurring in two stages: first the formation of a vacancy, and then its decay. The redistribution of energy between the photoelectron and the Auger electron links these two stages into a unitary process. As an example, the results of calculations[147,150,151] of the shift in energy and width of the Auger line $L_{2,3} \to M_{2,3}M_{2,3}$ in Ar, together with the experimental data,[144] shows that the influence of the post-collision interaction on the ionization process is manifested most strongly near the threshold, and declines with increasing photon energy.

Taking account of vacancy decay also alters the partial photoionization cross sections in the vicinity of the threshold of an ionizable shell. The additional attraction caused by the decay of the vacancy j to form two (or more) vacancies can lead even to capture of the slow photoelectron by discrete levels of the residual ion. Here the amplitude of (5.6) and (5.7) will describe the probability of single ionization above the threshold for formation of an inner vacancy j as $\tilde{\varepsilon} \to nl$. Thus, a calculation by (5.7) of the single-ionization cross section in the vicinity of the threshold of the $2p^6$ shell of Ar led to a maximum[57,149] observable experimentally.[143] At the same time, the single-ionization cross section calculated while neglecting the post-collision interaction and taking account of the influence of the $2p^6$ shell on the outer $3s^2$ and $3p^6$ electrons has a shallow minimum instead of a maximum.[57,149] We note here that the width of the maximum in the cross section σ^+ is much larger than the width of the 2p level itself.

For large Γ_j, i.e., small readjustment times $\tau_j \ll t$, one can assume a vacancy to decay instantaneously, while the motion of the ejected photoelectron is now treated in the field of the doubly charged ion that has undergone static readjustment. In this simplified model the photoionization cross section is proportional to the square of the dipole amplitude:

$$\sigma \sim |\langle \tilde{\varepsilon}_0 | \hat{D} | j \rangle|^2. \quad (5.8)$$

Here $\langle \tilde{\varepsilon}_0 |$ is the wave function of the electron in the field of the doubly charged ion. Concrete calculations of the photoionization cross sections of deep shells have shown that such a crude model in a number of cases describes well the experimental data, in particular for $1s^2$ of Ar.[152]

5.3. Mixing of vacancies. The spectroscopic factor

Thus far in Sec. 5 we have been treating the influence of readjustment of the core on the behavior of the ejected elec-

tron and the corresponding change in the ionization amplitude. Here we assumed that the created vacancy is a "pure" single-electron state. However, for inner shells, especially for those having weak transitions, this assumption is often incorrect, and strong mixing of more complex configurations exerts a considerable influence on the photoionization cross sections.[153] A vacancy created in the inner shells owing to configuration interaction amounts to a complex atomic excitation, in which the electrons of the outer shells also participate, as well as the electrons of the given shell. The quantity equal to the fraction of the pure single-electron state with the given vacancy in the complex excitation being treated is called the spectroscopic factor of the level F ($F<1$).[57,153] The fraction of the more complex states being mixed in is naturally $1-F$. The appearance of the spectroscopic factor arises from the dependence of the eigenenergy component Σ of the vacancy on the energy. The photoionization amplitude taking account of the eigenenergy component of the vacancy can be written as follows:

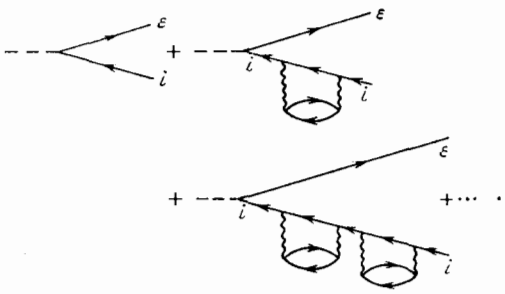

(5.9)

As a rule, it proves sufficient to take Σ in the lowest approximation (in the second order in the interelectronic interaction). The succession of diagrams of (5.9) enables one to take account of the deviation of the ionization potential from the single-particle value owing to readjustment of the ion caused by appearance of a vacancy and mixing of the pure hole state with more complex excitations of the type "two holes + one particle." The photoionization cross section determined by the amplitude of (5.9) can be written in the form[57]

$$\sigma(\omega)=\sigma_i(\omega)\left(1-\frac{\partial\Sigma}{\partial\varepsilon}\bigg|_{\varepsilon=\varepsilon_i}\right)^{-1}\equiv F_i\sigma_i(\omega). \qquad (5.10)$$

Here $|\varepsilon_i|=I_i$ is the ionization potential, and $\sigma_i(\omega)$ is the cross section in the single-particle approximation.

Taking account of Σ along with the intershell interactions amounts to a rather complicated problem. However, if the spectroscopic factor F of the shell acting on the shell being studied differs little from unity (and it usually happens thus for shells having strong transitions), the influence of the spectroscopic factor of the shell being ionized also can be taken into account by using (5.10).[57] Here, instead of the ionization cross section in the single-electron approximation $\sigma_i(\omega)$, one substitutes the cross section obtained with allowance for intershell correlations.

In particular, this is how one must find the ionization cross section of the ns^2 shells of the noble-gas atoms, for which F_{ns} differs from unity strongly.[154] Thus, for example, for Xe we have $F_{5s}=0.34$, and for Ar $F_{3s}=0.6$. The concrete calculations for Xe showed that a $5s^{-1}$ vacancy mixes most strongly with the states $5p^{-2}5d$ and $4d^{-2}\varepsilon f$, i.e., with excitations in adjoining shells, which make the main contribution to σ_{5s}. Taking account of F_{5s} in Xe by Eq. (5.10) leads to agreement of calculation with experiment in the energy region beyond the Cooper minimum, but it breaks down this agreement in the near-threshold region. However, we must take account of the fact that a mixing of configurations that leads to an appreciable deviation of F from unity alters the intershell interaction itself.[155] The matrix elements that govern the change in the interaction between the single-electron states can be written in the simplest case in the form

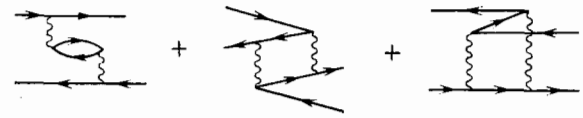

(5.11)

The diagrams of (5.11) are called "two particle-two hole" excitations. Taking them into account[155] enhances the influence of adjacent electron shells and compensates the decrease in σ_{5s} owing to appearance of the factor F_{5s}. With increasing ω, the influence of the "two particle-two hole" state rapidly declines, and the cross section is determined by (5.10). Curve *4* in Fig. 6, which agrees well with the experimental data throughout the energy range, specifically has been obtained by taking account of the intershell interaction and mixing of configurations.[57,62]

At large photon energies the role of the interactions in which the photoelectron participates declines. Hence the correlations, apart from those taken into account in the eigenenergy component Σ of the vacancy, become inessential. Thus, when $\omega\gg I_{ns}$, the cross section σ_{ns} is determined by (5.10).

5.4. "Shadow" levels. Collectivization of shells

The mixing of a vacancy in the nl shell with other states of the atom means that only a certain fraction ($F<1$) of the intensity of the initial level is manifested directly in the ionization of this level. The remaining intensity of the level $(1-F_{nl})$ is transferred to the states with which mixing occurs. Since the direct excitation of the latter in the ionization process is usually improbable, owing to their more complex structure, the mixing of the original level nl into these states mainly governs their "creation." In a certain sense such states become the "shadow" of nl, and hence such states have been called "shadow states."[57]

For example, one can assign to the "shadow" states the discrete excited state in Ar^+, $3p^{-2}3d$. Its strong interaction with a $3s^{-1}$ vacancy makes the main contribution to their mixing and determines the value of the spectroscopic factor of the $3s^{-1}$ level $F_{3s}\sim 0.6$.[154] Evidently the photoionization cross section of the neutral Ar atom to form a $3p^{-2}3d$ state must retain the features of the photoionization cross section of the $3s^2$ shell itself. If we neglect the intershell interaction between the np^6 and ns^2 shells, the following relationship holds for the cross sections if the shadow level is single[57]:

$$\sigma_{\tilde{n}s}(\omega)=\frac{1-F_{ns}}{F_{ns}}\sigma_{ns}(\omega). \qquad (5.12)$$

Here $\sigma_{\tilde{n}s}$ and σ_{ns} are the photoionization cross sections of the "shadow" and the original levels. However, the influence of the adjacent multielectron shells on the ionization of ns^2 is large, and since the ionization thresholds I_{ns} and $i_{\tilde{n}s}$ differ, the relationship between $\sigma_{\tilde{n}s}$ and $\sigma_{n\sigma}$ is not determined by the simple expression (5.12). A more accurate

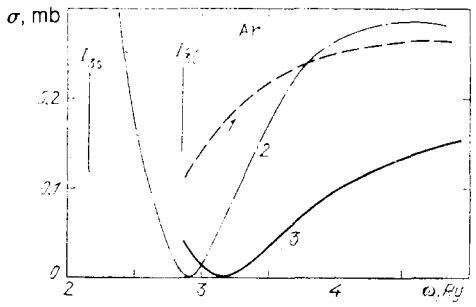

FIG. 21. Photoionization cross section with formation of $3s^{-1}$ and "shadow" $3\tilde{s} \to (3p^{-2}3d)$ states in Ar. *1*—$\sigma_{3\tilde{s}}$ in the Hartree-Fock approximation; *2*—σ_{3s} with allowance for the influence of the $3p^6$ shell; *3*—$\sigma_{3\tilde{s}}$ with allowance for the intershell interaction.[57]

calculation has been performed for the $\tilde{3}s \to (3p^{-2}3d)$ level in Ar.[57] As we see from Fig. 21, the photoionization cross section of this level resembles σ_{3s}. There are no experimental data on the photoionization of this level in Ar, but a satellite level has been found in the reaction of inelastic scattering of electrons (e, 2e),[156] which the authors interpreted as $3p^{-2}3d$.

We note that currently the ionization cross sections of satellite levels, including "shadow" levels, are being intensively studied experimentally and theoretically (in the noble-gas atoms, e.g., in Refs. 154, 157–159).

When the original level is mixed with several complex excitations or even with the continuous spectrum, they all jointly acquire the properties of shadow levels. Upon strong mixing with the continuous spectrum, the relationship (5.12) associates the cross sections for two- and one-electron photoionization. Here the original vacancy itself can lose a large part of its strength and individuality, and sometimes be fully collectivized. A striking example of this behavior of a vacancy is given by the study of the 4p shells in the atoms of Xe, Cs, Ba, and the following elements.[153,160] Especially distinguished is the behavior of the $4p_{1/2}$ level of Xe, for which even traces have not been detected in experiments on photoelectron and Auger spectroscopy.[161,162] This "disappearance" of a level is the manifestation of the very strong interaction of the $4p^{-1}$ state with the continuous spectrum of excitation of the 4d shell: $4d^{-2}\varepsilon f$, εp,[153] which leads to very rapid decay of the $4p_{1/2}^{-1}$ level and correspondingly to a great width $\Gamma_{4p} > 2\text{Ry}$. The spectroscopic factor $F_{4p_{1/2}}$ is close to zero. All this leads to "blurring" of the $4p_{1/2}^{-1}$ level, i.e., to its complete collectivization. In the photoelectron spectrum in the vicinity of its expected excitation energy, one observes a broad region of a continuous energy distribution of photoelectrons instead of the maximum usual for atomic levels.[160] Therefore, in determining the photoionization cross section in this energy region one must calculate the amplitude of the transition to the states of the continuous spectrum $4d^{-2}\varepsilon f$, εp.

In contrast to a $4p_{1/2}^{-1}$ vacancy, the maximum at a binding energy $E \approx 10.6$ Ry might be attributed to the $4p_{3/2}^{-1}$ level in the photoelectron spectrum. However, as a more detailed analysis shows,[153,160] this maximum corresponds mainly to the discrete state $4d^{-2}4f$, with which the $4p_{3/2}^{-1}$ vacancy interacts strongly. The remaining part of its strength has been taken up by excitations to the continuous spectrum $4d^{-2}\varepsilon f$. Thus the $4p_{3/2}^{-1}$ level also is fully collectivized under the influence of the 4d electrons.

To a great extent the $4s^{-1}$ level is also collectivized by strong interaction with the 4p and 4d electrons.[160] In the elements following Xe, the 4s and 4p levels also strongly mix with the states of the discrete and continuous spectra of the $4d^{10}$ shell.[153]

6. CONCLUSION

The strong action of one multielectron shell of an atom on another, whose amplitude in a state of the discrete and continuous spectra is relatively small, is manifested in the absolute majority of the atoms of the periodic system of elements. The intershell interaction is also substantial in many other processes besides those discussed above that involve the electronic structure of atoms. This pertains to the interaction of radiation, not only with isolated atoms, but also with multiatom structures existing in chemical compounds, clusters, and condensed media. In principle, the mechanism of interaction is everywhere the same, although in each individual case it has its specifics. The electrons of the outer shells substantially change their state also in passing from one atom to another, both owing to the interaction with the electrons of adjacent atoms and when the atoms enter into a chemical bond and form solids. The change in the state of the outer electrons strongly affects their influence on the deeper electron shells of atoms. Yet the states of the electrons of the inner shells in most cases change weakly. Therefore, if their influence on the outer electrons of an isolated atom is large, then it is large in any other analog of the outer shell, e.g., in the conduction band or the valence band. In this sense the action of the inner shells is more general in character and, as a rule, is manifested in ionization processes.

In this review we have mainly treated the manifestations of intershell interaction in neutral atoms, since as yet they have been studied clearly insufficiently in positive ions. However, evidently the influence of the adjacent shells on the shell being studied must decline with increasing charge because the energy of interaction of the electrons with the nucleus will substantially exceed the interaction energy among the electrons.

In closing we note also a set of photoprocesses in atoms and other objects not treated above and illustrating the manifestation of the intershell interaction.

6.1. Double ionization

The ejection of two electrons upon absorption of a single photon arises from the interelectron interaction. Usually the cross section σ^{++} for double photoionization is substantially smaller than that for single ionization σ^{+}. In light atoms where the interelectron correlations are small, we find the ratio $\sigma^{++}/\sigma^{+} \lesssim 0.04$.[163–165] However, for heavier atoms this ratio increases, and in the energy region where the influence of the inner shell is large, it becomes of the order of unity, and sometimes even larger.[166–169] The mechanism of increase of the probabilities of single and double photoionization is the same in principle in this case. The inner multielectron shell plays the role of a resonator, since it amplifies the electromagnetic field acting on the outer electrons upon absorbing an incident photon. The amplified oscillations of the field in which all the outer electrons move easily "shake

off" one or two electrons into the continuous spectrum if the photon energy suffices for this. Theoretical calculations of σ^{++} have as yet been performed only for light atoms.[164,165] Therefore one can decide on the role of the intershell interaction only from processing the experimental data.[167]

6.2. Photoionization of excited atoms

The influence of the inner shells affects the behavior of all the outer shells, the latter possibly including electrons lying in excited states. Since the spatial and energy intervals separating the excited electron from the remaining atomic electrons are also increased, on the whole we should expect the influence on it of the interaction with the inner shells to weaken. Nevertheless, with a large enough dynamic polarizability of the inner shell, its influence on the transition amplitudes of the excited electron can remain substantial. This is confirmed by the results of Ref. 170, which studied experimentally and theoretically the photoionization cross section of an electron excited to the 5d level in the Ba atom (Fig. 22). For photon energies close to the threshold of the $4d^{10}$ shell, the direct ionization of the 5d electrons is very small, while the appreciable maximum in the vicinity of $\omega \sim I_{4d}$ arises from the influence of the $4d^{10}$ electrons.

Studies of the ionization of atoms existing in excited states make it possible to obtain interesting information on the variation of the intershell interaction as a function of the distance of removal of one or several excited electrons from the core and of the principal quantum numbers of the levels and their angular momenta.

6.3. The influence of outer shells in ions and molecules

The influence of an outer shell on the ionization of a deeper shell can prove substantial, not only in atoms, but also in negative ions, molecules, and clusters when the behavior of the outer electrons does not differ too much from the atomic behavior.

Thus, a calculation within the ARPE framework of the cross section for photodetachment of 5s electrons in the negative ion I^- has shown[171] that the influence of the outer $5p^6$ shell is manifested even more strongly than in Xe, which has the same electronic structure. Since in most molecules containing iodine the latter enters in a state close to the negative ion, one can state that the influence of the outer electrons will be manifested also in these molecules.

Calculations have recently been performed of the photoionization cross sections of the hydrogen-containing molecules CH_4 and SiH_4,[172] which have "neon-like" and "argon-like" electronic structures. The calculations[172] showed that the outer molecular shell (an analog of np^6 in Ne and Ar) strongly alters the amplitude and cross section for photoionization of the deeper shell, which is an analog of ns^2 in Ne and Ar.

6.4. Photoionization of solids

For atoms existing in condensed states, the analog of the outer shell is the conduction or the valence band. Measurements of their partial photoionization cross sections in solids enable one to determine the features of the influence of the inner shells of atoms on the collectivized, delocalized electrons and to compare it with the influence on the bound electrons. This program is only beginning to be carried out, and the first results have been obtained on the photoionization of the 3d transition metals[173] and the rare-earth elements.[44,46,47] The greatest attention of investigators has been attracted to the region of photon energies close to the ionization threshold of the $4d^{10}$ shell (which, as we have seen from the previous examples, is the most convenient object for studying the intershell interaction). In particular, the experimental data given in Fig. 20 for the photoionization cross section of the 5p electrons were obtained in solid polycrystalline Ba.[44] Resonance amplification has been obtained in a crystal of LaB_6 [46] owing to the influence of the $4d^{10}$ shell and to the photoionization cross sections of the 5s, 5p, and 5d electrons in La. The same has been found also in the rare-earth metals,[46] including the electrons of the conduction band. We see from Fig. 23, which gives the experimental data on the partial cross sections in metallic Ce, that, although the influence of the $4d^{10}$ shell on the conduction electrons is smaller than on the bound electrons, specifically it determines the magnitude of the cross section at these energies. A comparison with the atomic calculations has shown[47,80] that in the first approximation the photoionization cross sections of the band electrons in these metals coincide with the corresponding cross sections in the isolated atom.

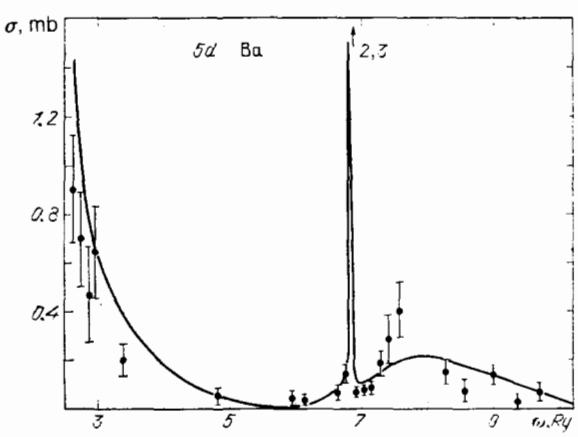

FIG. 22. The cross section σ_{5d} in Ba in the vicinity of the ionization threshold of the $4d^{10}$ shell.[170]

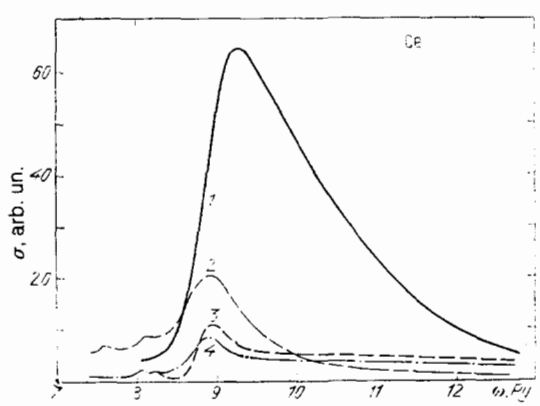

FIG. 23. Partial cross sections σ_i for photoionization of metallic Ce.[47] *1*—cross section of the $4d^{10}$ shell; *2*—cross section of the $5p^6$ shell; *3*, *4*—contributions of different bands.

The examples discussed in this review do not exhaust the different manifestations of the intershell interaction in atoms. We have restricted the treatment mainly only to photoionization processes, which have become one of the fundamental methods of studying the structure of matter upon the appearance of new, powerful sources of continuous-spectrum electromagnetic radiation—synchrotrons and accumulators. In this review we have not touched on the processes of radiative and Auger decay of vacancies, in which the intershell interaction often also plays a decisive role. Both the decay of vacancies and each of the examples listed in the Conclusion amount in principle to a broad and as yet poorly studied field of activity in atomic physics that has as its goal also the more exact determination of the structure of matter and the role in it of the interelectronic interaction.

[1)]Here and below in this article a shell is taken to mean a group of levels with a given principal quantum number n and orbital quantum number l.

[2)]Owing to the instability of a 4p vacancy, one actually cannot measure the cross-section σ_{4p} experimentally.

[1]D. R. Hartree, *The Calculation of Atomic Structures*, Wiley, N. Y. (1957) [Russ. transl., IL, M., 1960].

[2]H. A. Bethe and E. E. Salpeter, *Quantum Mechanics of One- and Two-Electron Systems*, Springer Verlag, Berlin, 1958 [Russ. transl., Fizmatgiz, M., 1960].

[3]J. C. Slater, *Quantum Theory of Atomic Structure*, McGraw-Hill, New York, 1960, Vol. 1.

[4]U. Fano and J. W. Cooper, Rev. Mod. Phys. **40**, 441 (1968) [Russ. transl., Nauka, M., 1972].

[5]I. I. Sobel'man, *Introduction to the Theory of Atomic Spectra*, Pergamon Press, Oxford (1973) [Russ. original, Fizmatgiz, M., 1963].

[6]M. Ya. Amusia, N. A. Cherepkov, and S. I. Sheftel, Phys. Lett. A **27**, 541 (1967).

[7]M. Ya. Amus'ya, N. A. Cherepkov, and L. V. Chernysheva, Zh. Eksp. Teor. Fiz. **60**, 160 (1971) [Sov. Phys. JETP **33**, 90 (1971)].

[8]H. P. Kelly and R. L. Simons, Phys. Rev. Lett. **30**, 529 (1973).

[9]P. G. Burke and K. T. Taylor, J. Phys. B **2**, 2620 (1975).

[10]T. N. Chang, Phys. Rev. A **15**, 2392 (1977).

[11]J. R. Swanson and L. Armstrong, Jr., *ibid.* **15**, 661 (1977); **16**, 1117 (1977).

[12]M. Ya. Amusia, V. K. Ivanov, N. A. Cherepkov, and L. V. Chernysheva, Phys. Lett. A **40**, 361 (1972).

[13]M. Ya. Amus'ya, V. K. Ivanov, N. A. Cherepkov, and L. V. Chernysheva, Zh. Eksp. Teor. Fiz. **66**, 1537 (1974) [Sov. Phys. JETP **39**, 752 (1974)].

[14]A. F. Starace, Handbuch der Physik, Springer Verlag, Berlin, 1982, Vol. 31, p. 1.

[15]A. A. Abrikosov, L. P. Gor'kov, and I. E. Dzyaloshinskiĭ, *Methods of Quantum Field Theory in Statistical Physics*, Prentice-Hall, Englewood Cliffs, N. J. (1963) [Russ. original, Fizmatgiz, M., 1962].

[16]M. Ya. Amusia and N. A. Cherepkov, Case Stud. At. Phys. **5**, 47 (1975).

[17]H. P. Kelly, Atomic Physics 2: Proc. 2nd Int. Conference on Atomic Physics, Plenum Press, London, 1971, p. 227.

[18]H. R. Kelly, Phys. Scripta **21**, 448 (1980).

[19]W. R. Johnson, C. D. Lin, and K. T. Cheng, *ibid.*, p. 409.

[20]W. R. Johnson and G. Soff, Phys. Rev. Lett. **50**, 1361 (1983).

[21]L. J. Armstrong and W. R. J. Fielder, Phys. Scripta **21**, 457 (1980).

[22]T. N. Chang and U. Fano, Phys. Rev. A **13**, 263 (1976).

[23]A. Zangwill and P. Soven, *ibid.* **21**, 1561 (1980); A. Zangwill, Atomic Physics 8: Proc. 8th ICAP, Plenum Press, London, 1983, p. 339.

[24]J. J. Chang, J. Phys. B **10**, 3195 (1977).

[25]F. A. Parpia and W. R. Johnson, *ibid.* **17**, 531 (1984).

[26]J. A. R. Samson, see Ref. 14, p. 123.

[27]I. B. Bersuker, Dokl. Akad. Nauk SSSR **113**, 1017 (1957) [Sov. Phys. Dokl. **2**, 167 (1958)]; Opt. Spektrosk. **3**, 97 (1957).

[28]W. R. Johnson, V. Radojevic, J. C. Desmukh, and K. T. Cheng, Phys. Rev. A **25**, 337 (1982).

[29]V. L. Carter, R. D. Hudson, and B. L. Breig, *ibid.* **4**, 821 (1971).

[30]W. R. Johnson and P. C. Desmukh, *ibid.* **27**, 326 (1983).

[31]J. P. Connerade, M. A. Baig, W. R. S. Carton, and G. H. Newson, Proc. R. Soc. London Ser. A **371**, 295 (1980).

[32]Z. Altun, S. L. Carter, and H. P. Kelly, J. Phys. B **15**, L709 (1982); Phys. Rev. A **23**, 1947 (1983).

[33]P. Scott, A. E. Kingston, and A. Hibbert, J. Phys. B **16**, 3945 (1983).

[34]G. V. Marr and J. M. Austin, *ibid.* **2**, 168 (1972).

[35]S. P. Shannon and K. Codling, *ibid.* **11**, 1193 (1978).

[36]P. H. Kobrin, U. Becker, S. Southworth, C. M. Truesdale, D. W. Lindle, and D. A. Shirley, Phys. Rev. A **26**, 842 (1982).

[37]V. K. Ivanov, S. Yu. Medvedev, and V. A. Sosnivker, Preprint of the PTI Akad. Nauk SSSR No. 615, Leningrad, 1979; Opt. Spektrosk. **58**, 749 (1985) [Opt. Spectrosc. (USSR) **58**, 457 (1985)].

[38]M. Ya. Amusia, N. A. Cherepkov, I. Pavlin, and V. Radojevic, Phys. Rev. A **13**, 146 (1976).

[39]M. Ya. Amusia, N. A. Cherepkov, I. Pavlin, V. Radojevic, and Dj. Zivanovic, J. Phys. B **10**, 1413 (1977).

[40]P. C. Desmukh and S. T. Manson, Phys. Rev. A **28**, 209 (1983).

[41]M. Ya. Amusia and V. K. Ivanov, Phys. Lett. A **59**, 194 (1976).

[42]M. J. Van der Wiel and G. R.Wight, *ibid.* **54**, 83 (1975).

[43]J. B. West, P. R. Woodruff, K. Codling, and R. G. Houlgate, J. Phys. B **9**, 407 (1976).

[44]M. H. Hecht and I. Lindau, Phys. Rev. Lett. **47**, 821 (1981).

[45]M. Ya. Amus'ya, V. K. Ivanov, S. A. Sheĭnerman, and S. I. Sheftel', Zh. Eksp. Teor. Fiz. **78**, 910 (1980) [Sov. Phys. JETP **51**, 458 (1980)].

[46]M. Aono, T.-C. Chiang, F. J. Himpsel, and D. E. Eastman, Solid State Commun. **37**, 471 (1981).

[47]F. Gerken, J. Barth, and C. Kunz, Preprint DESY SR-82-13, Hamburg, 1982.

[48]M. J. Lynch, J. L. Gardner, K. Codling, and G. V. Marr, Phys. Lett. A **43**, 237 (1973).

[49]J. A. R. Samson and J. L. Gardner, Phys. Rev. Lett. **33**, 671 (1974).

[50]F. Wuilleumier and M. O. Krause, Phys. Rev. A **10**, 242 (1974).

[51]R. G. Houlgate, J. B. West, K. Codling, and G. V. Marr, J. Phys. A **7**, L470 (1974); J. Electron Spectr. and Rel. Phenom. **9**, 205 (1976).

[52]K. H. Tan and C. E. Brion, *ibid.* **13**, 77 (1978).

[53]C. D. Lin, Phys. Rev. A **9**, 171 (1974).

[54]T. N. Chang, *ibid.* **18**, 1448 (1978).

[55]W. R. Johnson and K. T. Cheng, *ibid.* **20**, 978 (1979).

[56]K. Codling, R. G. Houlgate, J. B. West, and P. R. Woodruff, J. Phys. B **9**, L83 (1976).

[57]M. Ya. Amusia, Adv. At. Mol. Phys. **17**, 1 (1981).

[58]M. Y. Adam, N. Wuilleumier, N. Sandner, S. Krummacher, V. Schmidt, and W. Mehlhorn, Jpn. J. Appl. Phys. **17**, 170 (1978).

[59]T. Gustafsson, Chem. Phys. Lett. **51**, 383 (1977).

[60]A. Fahlman, T. A. Carlson, and M. O. Krause, Phys. Rev. Lett. **50**, 1114 (1983).

[61]K.-N. Huang and A. F. Starace, Phys. Rev. A **21**, 697 (1980).

[62]V. L. Sukhorukov, I. D. Petrov, V. F. Demekhin, and S. V. Lavrent'ev, Izv. Akad. Nauk SSSR Ser. Fiz. **49**, 1463 (1985) [Bull. Acad. Sci. USSR Phys. Ser. **49**(8), 6 (1985)].

[63]M. Inokuti, Rev. Mod. Phys. **43**, 297 (1971).

[64]M. Ya. Amusia, V. K. Ivanov, and S. A. Sheinerman, J. Phys. B **9**, 1537 (1976).

[65]J. L. Dehmer and J. Berkowitz, Phys. Rev. A **10**, 484 (1974).

[66]J. A. R. Samson, J. L. Gardner, and A. Starace, *ibid.* 12, 1459 (1975).

[67]F. Wuilleumier, M. Y. Adam, P. Dhez, N. Sandner, V. Schmidt, and W. Mehlhorn, *ibid.* **16**, 646 (1977).

[68]F. Wuilleumier, M. Y. Adam, N. Sandner, V. Schmidt, W. Mehlhorn, and J. P. Desclaux, Proc. 5th Intern. Conference on VUV Physics, Montpellier, France, 1977, p. 41.

[69]S. P. Shannon, K. Codling, and J. B. West, J. Phys. B **10**, 825 (1977).

[70]W. Ong and S. T. Manson, J. Phys. B **11**, L163 (1978); Phys. Rev. A **21**, 842 (1980).

[71]B. H. Brandow, Rev. Mod. Phys. **39**, 771 (1967).

[72]V. V. Tolmachev, Theory of the Fermi Gas (in Russian), Izd-vo Mosk un-ta, M., 1973, p. 354.

[73]I. Lindgren, J. Phys. B **7**, 2441 (1974).

[74]K. T. Taylor and P. G. Burke, *ibid.* **9**, L353 (1976).

[75]L. Armstrong, *ibid.* 7, 2320 (1974).

[76]N. A. Cherepkov and L. V. Chernysheva, Izv. Akad. Nauk SSSR Ser. Fiz. **41**, 2518 (1977) [Bull. Acad. Sci. USSR Phys. Ser. **41**(12), 47 (1977)].

[77]A. F. Starace and L. Armstrong, Phys. Rev. A **13**, 1850 (1976).

[78]E. R. Brown, S. L. Carter, and H. P. Kelly, Phys. Lett. A **66**, 290 (1978); Phys. Rev. A **21**, 1237 (1980).

[79]M. Lemoureux and F. C. Farnoux, J. Phys. (Paris) **40**, 545 (1979).

[80]A. Zangwill and P. Soven, Phys. Rev. Lett. **45**, 204 (1980).

[81]M. Ya. Amus'ya, V. K. Dolmatov, and V. K. Ivanov, Zh. Eksp. Teor. Fiz. **85**, 115 (1983) [Sov. Phys. JETP **58**, 67 (1983)].

[82]K.-N. Huang and A. F. Starace, Phys. Rev. A **20**, 318 (1980).

[83]E. R. Watson and A. J. Freeman, Phys. Rev. **120**, 1125 (1960).

[84]C. S. Fadley, D. A. Shirley, A. J. Freeman, P. S. Bagus, and J. V. Mallow, Phys. Rev. Lett. **23**, 1397 (1969).

[85]I. L. Beĭgman, L. A. Vaĭnshteĭn, and V. P. Shevel'ko, Opt. Spektrosk. **28**, 425 (1970) [Opt. Spectrosc. (USSR) **28**, 229 (1979)].

[86]R. L. Smith and R. W. Labahn, Phys. Rev. A **2**, 2317 (1970).

[87]J. C. Weisheit, *ibid.* A **5**, 1621 (1972).

[88]D. W. Norcross, *ibid.* A **7**, 606 (1973).
[89]R. W. Labahn and E. A. Garbaty, *ibid.* **9**, 2255 (1974).
[90]R. D. Hudson and L. J. Kieffer, At. Data **2**, 205 (1971).
[91]G. V. Marr and D. M. Creek, Proc. R. Soc. London Ser. A **304**, 233 (1968).
[92]T. B. Cook, F. B. Dunning, G. W. Foltz, and R. F. Stebbings, Phys. Rev. A **15**, 1526 (1977).
[93]T. N. Chang, J. Phys. B **8**, 743 (1975).
[94]J. J. Chang and H. P. Kelly, Phys. Rev. A **12**, 92 (1975).
[95]S. T. Manson, A. Msezane, A. F. Starace, and S. Shahabi, *ibid.* **20**, 1005 (1979).
[96]J. P. Connerade, M. W. D. Mansfield, and M. A. P. Martin, Proc. R. Soc. London Ser. A **350**, 405 (1976).
[97]R. Bruhn, B. Sonntag, and H. W. Wolff, Phys. Lett. A **69**, 9 (1978).
[98]R. Bruhn, H. Schmidt, H. Schröder, and B. Sonntag, *ibid.* **90**, 41 (1982).
[99]R. Bruhn, E. Schmidt, H. Schröder, and B. Sonntag, J. Phys. B **15**, 2807 (1982).
[100]E. Schmidt, H. Schröder, B. Sonntag, H. Voss, and H. E. Wetzel, *ibid.* **16**, 2961 (1983).
[101]L. C. Davis and L. A. Feldkamp, Solid State Commun. **19**, 413 (1976).
[102]M. Ya. Amus'ya, V. K. Dolmatov, and V. K. Ivanov, Pis'ma Zh. Tekh. Fiz. **4**, 1305 (1978) [Sov. Tech. Phys. Lett. 4, 525 (1978)]; M. Ya. Amusia, V. K. Ivanov, and L. V. Chernysheva, J. Phys. B **14**, L19 (1981).
[103]L. C. Davis and L. A. Feldkamp, Phys. Rev. A **17**, 2012 (1978).
[104]L. J. Garvin, E. R. Brown, S. L. Carter, and H. P. Kelly, J. Phys. B **16**, L269 (1983).
[105]M. A. Baig, J. P. Connerade, and G. H. Newson, Proc. R. Soc. London Ser. A **367**, 381 (1979).
[106]E. Schmidt, H. Schröder, B. Sonntag, H. Voss, and H. E. Wetzel, J. Phys. B **17**, 707 (1984); **18**, 79 (1985).
[107]P. H. Kobrin, U. Becker, C. M. Truesdale, D. W. Lindle, H. G. Kerkhoff, and D. A. Shirley, J. Electron. Spectr. Rel. Phenom. **34**, 129 (1984).
[108]M. O. Krause, T. A. Carlson, and A. Fahlman, Phys. Rev. A **30**, 1316 (1984).
[109]R. Malutzki, M. S. Banna, W. Braun, and V. Schmidt, J. Phys. B **18**, 1735 (1985).
[110]V. Schmidt, Commun. At. Mol. Phys. **17**, 1 (1985).
[111]T. M. Zimkina, V. A. Fomichev, S. A. Gribovskiĭ, and I. I. Zhukova, Fiz. Tverd. Tela (Leningrad) **9**, 1447, 1490 (1967) [Sov. Phys. Solid State **9**, 1128, 1163 (1967)].
[112]M. Ya. Amusia and S. L. Sheftel, Phys. Lett. A **55**, 469 (1976).
[113]J. Cooper and R. N. Zare, J. Chem. Phys. **48**, 942 (1968).
[114]M. Ya. Amus'ya and V. K. Ivanov, Izv. Akad. Nauk SSSR Ser. Fiz. **41**, 2509 (1977) [Bull. Acad. Sci. USSR Phys. Ser. **41**(12), 39 (1977)].
[115]M. Lynch, K. Codling, and A. Gardner, Phys. Lett. A **43**, 213 (1973).
[116]J. L. Dehmer, W. A. Chupka, J. Berkowitz, and W. T. Jivery, Phys. Rev. A **12**, 1966 (1975).
[117]L. Torop, J. Morton, and J. B. West, J. Phys. B **9**, 2035 (1976).
[118]M. O. Krause, T. A. Carlson, and P. R. Woodruff, Phys. Rev. A **24**, 1374 (1981).
[119]S. Southworth, U. Becker, C. M. Truesdale, P. H. Kobrin, D. W. Lindle, S. Owaki, and D. A. Shirley, *ibid.* **28**, 261 (1983).
[120]M. Ya. Amusia, L. V. Chernysheva, and S. A. Sheinerman, Phys. Lett. A **82**, 171 (1981).
[121]S. T. Manson and A. F. Starace, Rev. Mod. Phys. **54**, 389 (1982).
[122]K.-N. Huang, W. R. Johnson, and K. T. Cheng, At. Data Nucl. Data Tables **26**, 33 (1981).
[123]D. Dill, Phys. Rev. A **7**, 1976 (1973).
[124]N. A. Cherepkov, Phys. Lett. A **66**, 204 (1978).
[125]A. Fahlman, T. A. Carlson, and M. O. Krause, J. Phys. B **16**, L485 (1983).
[126]H. Derenbach and V. Schmidt, *ibid.* **17**, 83 (1984).
[127]J. L. Dehmer and D. Dill, Phys. Rev. Lett. **37**, 1049 (1976).
[128]M. G. White, S. H. Southworth, P. Kobrin, E. D. Poliakoff, R. Rosenberg, and D. A. Shirley, *ibid.* **43**, 1661 (1979).
[129]H. Derenbach and V. Schmidt, J. Phys. B **16**, L337 (1983).
[130]Y. S. Kim, R. H. Pratt, A. Ron, and H. Tseng, Phys. Rev. A **22**, 567 (1980).
[131]A. Niehaus and M. W. Ruf, Z. Phys. **252**, 84 (1972).
[132]G. Schonhence, U. Heinzmann, J. Kessler, and N. A. Sherepkov, Phys. Rev. Lett. **48**, 603 (1982).
[133]M. Ya. Amusia, V. K. Dolmatov, and V. K. Ivanov, J. Phys. B **16**, L753 (1983).
[134]N. A. Cherepkov, Zh. Eksp. Teor. Fiz. **65**, 933 (1973) [Sov. Phys. JETP **38**, 463 (1973)].
[135]C. M. Lee, Phys. Rev. A **10**, 1598 (1974).
[136]N. A. Cherepkov, J. Phys. B **12**, 1279 (1979).
[137]K.-N. Huang, Phys. Rev. A **22**, 223 (1980).
[138]U. Heinzmann, G. Schonhence, and J. Kessler, Phys. Rev. Lett. **42**, 1603 (1979).
[139]U. Heinzmann, J. Phys. B **13**, 4353 (1980).
[140]S. Flügge, W. Mehlhorn, and V. Schmidt, Phys. Rev. Lett. **29**, 7 (1972).
[141]E. C. Berezhko, N. M. Kabachnik, and V. S. Rostovsky, J. Phys. B **11**, 1749 (1978).
[142]E. G. Berezhko, V. K. Ivanov, and N. M. Kabachnik, Phys. Lett. A **66**, 474 (1978).
[143]M. J. Van der Wiel, G. R. Wight, and R. R. Tol, J. Phys. Ser. B **9**, L5 (1976).
[144]H. Hanashiro, Y. Suzuki, T. Sasaki, A. Mikuni, T. Takayanagi, K. Wakiya, H. Suzuki, A. Danjo, T. Hino, and S. Ohtani, *ibid.* **12**, L775 (1979).
[145]V. Schmidt, S. Krummacher, P. Wuilleumier, and P. Dhez, Phys. Rev. A **21**, 1803 (1981).
[146]F. H. Read, J. Phys. B **10**, L207 (1977).
[147]A. Niehaus, *ibid.*, p. 1845.
[148]M. Ya. Amusia, M. Yu. Kuchiev, S. A. Sheinerman, and S. I. Sheftel, *ibid.*, p. L535.
[149]V. N. Ostrovskiĭ, Zh. Eksp. Teor. Fiz. **72**, 2079 (1977) [Sov. Phys. JETP **45**, 1092 (1977)].
[150]K. Helenelund, S. Hedman, L. Asplund, U. Gelius, and K. Siegbahn, Phys. Scripta **27**, 245 (1983).
[151]M. Yu. Kuchiev and S. A. Sheinerman, J. Phys. B **18**, L551 (1984).
[152]M. Ya. Amusia, V. K. Ivanov, and V. A. Kupchenko, *ibid.* **14**, L667 (1981).
[153]G. Wendin, *Structure and Bonding*, Springer Verlag, Berlin, 1981, p. 1 (Springer Series of Solid State Sciences, Vol. 45).
[154]J. E. Hansen, Commun. At. Mol. Phys. **12**, 197 (1982).
[155]M. Ya. Amusia and A. S. Kheifets, Phys. Lett. A **82**, 407 (1981).
[156]I. E. McCarthy and E. Weigold, Adv. At. Mol. Phys. **14**, 127 (1978).
[157]A. Fahlman, M. O. Krause, T. A. Carlson, and A. Svensson, Phys. Rev. A **30**, 812 (1984).
[158]D. W. Lindle, P. A. Weimann, T. A. Ferret, P. H. Kobrin, C. M. Truesdale, U. Becker, H. Kerkhoff, and D. Shirley, *ibid.* **33**, 319 (1986).
[159]I. D. Petrov, V. L. Sukhorukov, V. F. Demekhin, and S. V. Lavrent'ev, Abstracts of Reports of the All-Union Conference on Quantum Chemistry and Solid-State Spectroscopy (in Russian), Sverdlovsk, 1986, p. 123.
[160]G. Wendin and M. Ohno, Phys. Scripta **14**, 148 (1976).
[161]U. Gelius, J. Electron. Spectr. Rel. Phenom. **5**, 985 (1974).
[162]S. Svensson, N. Martenson, E. Basilier, P. A. Malmquist, U. Gelius, and K. Siegbahn, Phy. Scripta **14**, 141 (1976).
[163]F. W. Byron and C. J. Joachain, Phys. Rev. **164**, 1 (1967).
[164]S. L. Carter and H. P. Kelly, Phys. Rev. A **21**, 170 (1981).
[165]M. Ya. Amusia, Commun. At. Mol. Phys. **4**, 155 (1981).
[166]J. A. R. Samson and G. N. Haddad, Phys. Rev. Lett. **33**, 875 (1974).
[167]M. J. Van der Wiel and T. W. Chang, J. Phys. B **11**, L125 (1978).
[168]J. P. Connerade, S. J. Rose, and I. P. Grant, *ibid.* **12**, 291 (1979).
[169]D. M. Holland, K. Codling, and R. N. Chamberlain, *ibid.* **14**, 839 (1981).
[170]J. M. Bizau, D. Cubayanes, P. Gerard, F. Wuilleumier, J. C. Keller, J. L. Le Gouet, J. Piqque, B. Carre, D. Ederer, and G. Wendin, Abstracts of Contributed Papers of the XIV ICPEAC, Palo Alto, USA, 1985, p. 7.
[171]M. Ya. Amus'ya, G. F. Gribakin, V. K. Ivanov, and L. V. Chernysheva, Izv. Akad. Nauk SSSR Ser. Fiz. **50**, 1274 (1986) [Bull. Acad. Sci. USSR Phys. Ser. **50**(7), 26 (1986)].
[172]V. L. Sukhorukov, S. V. Lavrent'ev, V. F. Demekhin, and I. D. Petrov, Khim. Fizika **3**, 359 (1984).
[173]J. Barth, F. Gerken, and C. Kunz, Phys. Rev. B **31**, 2022 (1985).

Translated by M. V. King